Front. Mech. Eng. 2025, 20(2): 15
https://doi.org/10.1007/s11465-025-0833-7

REVIEW ARTICLE

Review of damping composite materials and structures involving self-healing constituents

Haibo FENG, Li LI (✉)

State Key Laboratory of Intelligent Manufacturing Equipment and Technology, School of Mechanical Science and Engineering, Huazhong University of Science and Technology, Wuhan 430074, China

✉ Corresponding author. Email: lili_em@hust.edu.cn (Li LI)

ABSTRACT The continuous pursuit of extremely lightweight and multi-functional integrated designs in modern industries requires that structural materials are not limited to ensuring the structural load-bearing function of lightweight designs; rather, they must have high mechanical properties and high damping capabilities. Self-healing materials are becoming popular because of their attractive repairability and reprocessability. Dynamic reversible bonds, which are included in self-healing polymer networks, have been extensively studied with respect to different chemical mechanisms. Nevertheless, the ability to reach high stiffness and high damping performance is crucial. In this review, different types of self-healing materials are introduced, and their complex and contradictory relationships with stiffness, damping, and self-healing properties are explained. This review combines intrinsic damping sources and extrinsic deformation driving modes as a holistic concept of material–structure–performance integrated design methodology to address the extensive challenges of increasing specific damping performance. Specifically, the sources of damping at the nanolevel and the deformation-driving modes at different levels of structural hierarchy are explained in depth to reveal the cross-scale coordination between intrinsic damping sources and extrinsic deformation-driven modes originating from extremely different length scales in the microstructural architecture of a material. The material–structure–performance integrated design methodology is expected to become a key strategy for the sustainable development of breakthrough and transformative damping composite structures for aerospace, terrestrial, and marine transportation.

KEYWORDS bio-inspired self-healing materials, mechanical properties, damping mechanisms, multiscale, structural damping composites, hierarchy

1 Introduction

Structural components are the cornerstone of modern industries, such as the aviation, aerospace, navigation, automobile, and robot fields; they often operate in vibration environments. Damping is crucial to vibration-induced problems, including but not limited to instrument operation accuracy, vibration and noise control, equipment reliability, and service life of components (or machines).

With the continuous pursuit of extremely lightweight designs in some advanced high-tech industries and the rapid development in the direction of multi-functional integration, such as comfort and intelligence, new challenges have been posed to the engineering application of structural materials. This requires that structural materials are not limited to ensuring the structural load-bearing function in lightweight design but also require them to have high mechanical properties and high damping capabilities.

A structure–damping composite material (or structure) is the inevitable way to achieve the requirements of a superior integrated structure and damping performance. Classical structure–damping composite structures, including free-layer damping (FLD) treatment and constrained-layer damping (CLD) treatment (left side of Fig. 1), are widely used in modern industries, such as automobiles and commercial airplanes [1].

The FLD treatment, where a layer of viscoelastic damping material is attached to a base structure, is

Received October 26, 2024; accepted January 12, 2025; online April 23, 2025

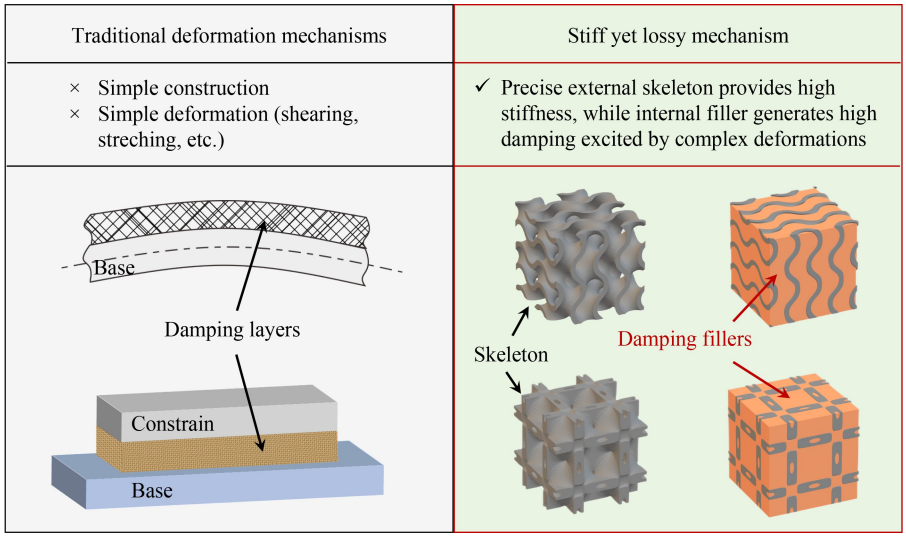

Fig. 1 Traditional and emerging damping treatments and their deformation mechanisms.

probably the most successful of the many approaches to designing structure and damping roles in engineering structures owing to its ease of fabrication. Damping layers upon a strong yet low-lossy base structure allows the attainment of strength and damping in the FLD treatment. The effective damping capability ($\tan\delta$) of the FLD treatment under tension/compression or bending excitation can be expressed as follows [2,3]:

$$\tan\delta \propto \frac{h_d}{h_b} \times \frac{E_d' \tan\delta_d}{E_b'}, \tag{1}$$

where the subscripts d and b denote the damping layer and the base structure, respectively; E' is the storage modulus; and h denotes the thickness of the damping layer or the base structure. According to Eq. (1), the effective damping capability depends not only on the damping of the damping layer but also on its stiffness (or modulus). This can be easily understood. For a damping material with high damping but low stiffness, low stiffness inevitably weakens the capability to store deformation-induced mechanical energy, which then means that the mechanical energy acting on the damping material is small; as a result, although high damping has excellent capabilities of mechanical energy dissipation, the total energy loss may also be small, and correspondingly, the effective (equivalent) damping of the entire mechanical system is low. However, a stiff yet lossy mechanism cannot be easily designed because of the conflict between stiffness and damping properties in traditional engineering materials. Blindly pursuing the highest performance of damping materials inevitably leads to unacceptably low stiffness performance. Although the mechanical energy dissipation process can be accelerated in the damping material itself, the equivalent damping capacity of the entire mechanical system involving the damping material eventually weakens rather than the opposite.

Although the quest continues for better lossy materials, these materials are nearly useless as damping materials without the appropriate ability to store mechanical energy. Therefore, in structural applications, a damping layer with high stiffness and high damping (specific damping performance) is desirable [4–6], and the pursuit of materials endowed with extremely specific damping has long been a major quest in aviation and aerospace engineering. Unfortunately, the stiffness and damping properties are generally mutually exclusive, and their product (figure of merit) has a limit for traditional engineering materials. With respect to this extremely challenging problem, the attainment of high stiffness and high damping has become a bottleneck hindering the improvement of the dynamic performance of machinery equipment, especially in aviation, aerospace, and navigation, which have extremely lightweight requirements.

In practical applications, when a high-damping material does not undergo mechanical deformation, the damping material does not store mechanical energy, and no energy dissipation occurs. That is, damping capability cannot be exerted without deformation of the damping layer. Various deformation mechanisms have been designed to solve the problem in which high-damping materials need mechanical energy to excite and dissipate energy. Traditional FLD and CLD treatments are based on stretching and shear deformation mechanisms, respectively. However, the damping capability of such treatments has good vibration and noise reduction effects only in specific deformation modes.

With the rapid development of additive manufacturing technology [7,8], complex configurations and their superior performance are no longer a daunting problem when material–structure–performance integrated manufacturing techniques are used. Thus, stiff yet lossy mechanisms can be explored in the design of hierarchical multiscale materials with carefully complex crafted microstructures; examples include the metamaterials shown on the right side of Fig. 1. When "external rigidity but internal chaos" deformation modes are designed, rational design methods, such as the topology optimization-based design method, can be employed to generate complex crafted microstructures. The incomplete theoretical understanding of damping in multiscale materials limits the ability of rational design methods. In terms of easing the theoretical concern, biomimetic design methods and machine learning-based design methods seem logical in generating highly complex crafted microstructures. These recently designed microstructures with "external rigidity but internal chaos" deformation modes (e.g., topology optimization-based microstructures, biomimetic microstructures, and machine learning-based multiscale hierarchical lattices or metamaterials) provide breakthrough and transformative alternatives to more traditional materials, such as traditional FLD and CLD treatments.

Polymeric materials with outstanding physical and mechanical properties have become the fourth largest aerospace material after aluminum, steel, and titanium alloys [9]. However, their non-reprocessability still limits the development of engineering applications. The recently proposed self-healing polymeric materials can prevent potentially catastrophic damage by intelligently repairing themselves, restoring all or most of the original properties, thus extending their life [10]. Owing to the reprocessability of self-healing polymeric materials, in contrast to traditional thermoset resins, they can be recycled and therefore reused. Furthermore, the self-healing property itself is a chemical reaction that requires the dissipation of energy, so it can be exploited to improve damping capabilities [11] (Fig. 2). Thus, self-healing polymeric materials can introduce a chemical damping mechanism driven by reversible chemical reactions, making them ideal structural damping materials.

Its practicality can also be highlighted by taking the vehicle industry as an example. Many steel-based structural components with damping-layer treatments in a truck, such as a tuned viscoelastic damper, insulators in brackets, spray dampers on floor panels, crossbeams, balanced suspensions, stand-off layer damping systems, and engine mounts, can find applications for damping composite structures involving self-healing constituents (Fig. 3). In addition to meeting the criteria for self-healing, mechanical and damping performance requirements, self-healing materials enable advanced manufacturing that achieves lightweight and integrated designs, thereby offering a new class of polymeric materials to replace traditional thermosetting resins [12,13].

As mentioned above, the effective damping performance of a damped composite structure relies not only on its intrinsic damping sources at the nanoscale but also on its extrinsic deformation-driving modes at the macroscale. However, most current research focuses either on intrinsic damping sources in materials science or on extrinsic deformation-driven modes in structural design. That is, the traditional route of designing effective damping performance is a material-performance integrated method that

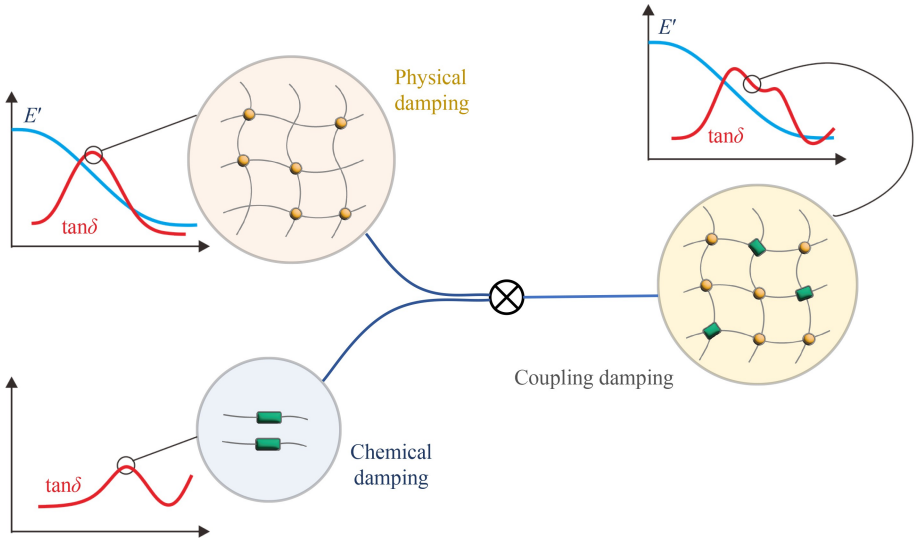

Fig. 2 Coupling damping performance of self-healing polymeric materials.

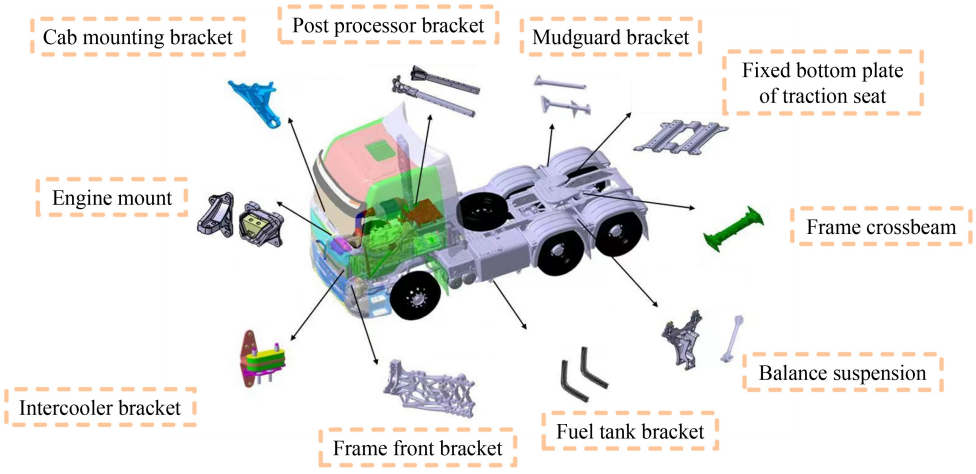

Fig. 3 Potential applications of damping composite structures involving self-healing constituents in a commercial vehicle.

improves material damping in a fixed structure or a structure-performance integrated method that designs structural damping under the condition of a fixed material damping property. This results in a tedious trial-and-error approach that creates challenges in achieving the goal of high specific damping performance.

This review combines intrinsic damping sources and extrinsic deformation driving modes as a holistic concept of material–structure–performance integrated design methodology to address the extensive challenges of increasing specific damping performance. Specifically, we focus on the self-healing constituents that have been proven to achieve a surpassingly stiff yet lossy performance. Learning from nature, the cross-scale coordination between intrinsic damping sources and extrinsic deformation-driven modes can originate from noticeably different length scales (millimeter- to meter-scale) in the microstructural architecture of composite structures. Therefore, the sources of damping at the nanolevel and the deformation-driving modes at different levels of structural hierarchy are explained in depth so that the underlying principles can be understood.

2 Self-healing materials

2.1 Combination of natural and engineering materials

The concept of self-healing materials started in 1990. Scientists were inspired by natural organisms such as humans and animals. When a minor accident occurs and a wound appears on the skin, blood flows out, but platelets quickly cause the blood to clot, thus allowing the wound to heal. The self-healing phenomenon also appears at the macroscopic level, such as the rebuilding of bones (Fig. 4), or at the molecular level, such as DNA repair [15]. Self-healing is a property of natural living organisms. Inspired by the natural world, self-healing materials have emerged and received a great deal of attention and development in engineering [16].

2.2 Self-healing approaches

2.2.1 Extrinsic self-healing

Self-healing materials have been designed to be extrinsic or intrinsic according to self-healing mechanisms [17]. Extrinsic self-healing materials are those in which the repair process depends on an external agent. Generally, microcapsule-based healing agents dispersed in the matrix are widely developed [18–23]. Figure 5 shows the insulating healing paint and solid catalysts encapsulated in the microcapsule, which can release liquid healing agents and repair cracks. The microcapsule shell must be chemically compatible with the healing agent, which should also have a long shelf life and a suitable sealing property. The microcapsule walls must be sufficiently resistant to the processing conditions of the matrix [24]. Hollow fibers or thermal epoxy particles can also act as encapsulation carriers to better match the properties of the fillers and matrix and contain a more significant volume of healing agent [25,26]. Another novel extrinsic self-healing mechanism relies on a vascular network system consisting of fibers or nanotubes. Similarly, a large amount of repair fluid in the tube is widely distributed in the structure, but it can repair all types of composite failure modes at any point in the structure without destroying some major

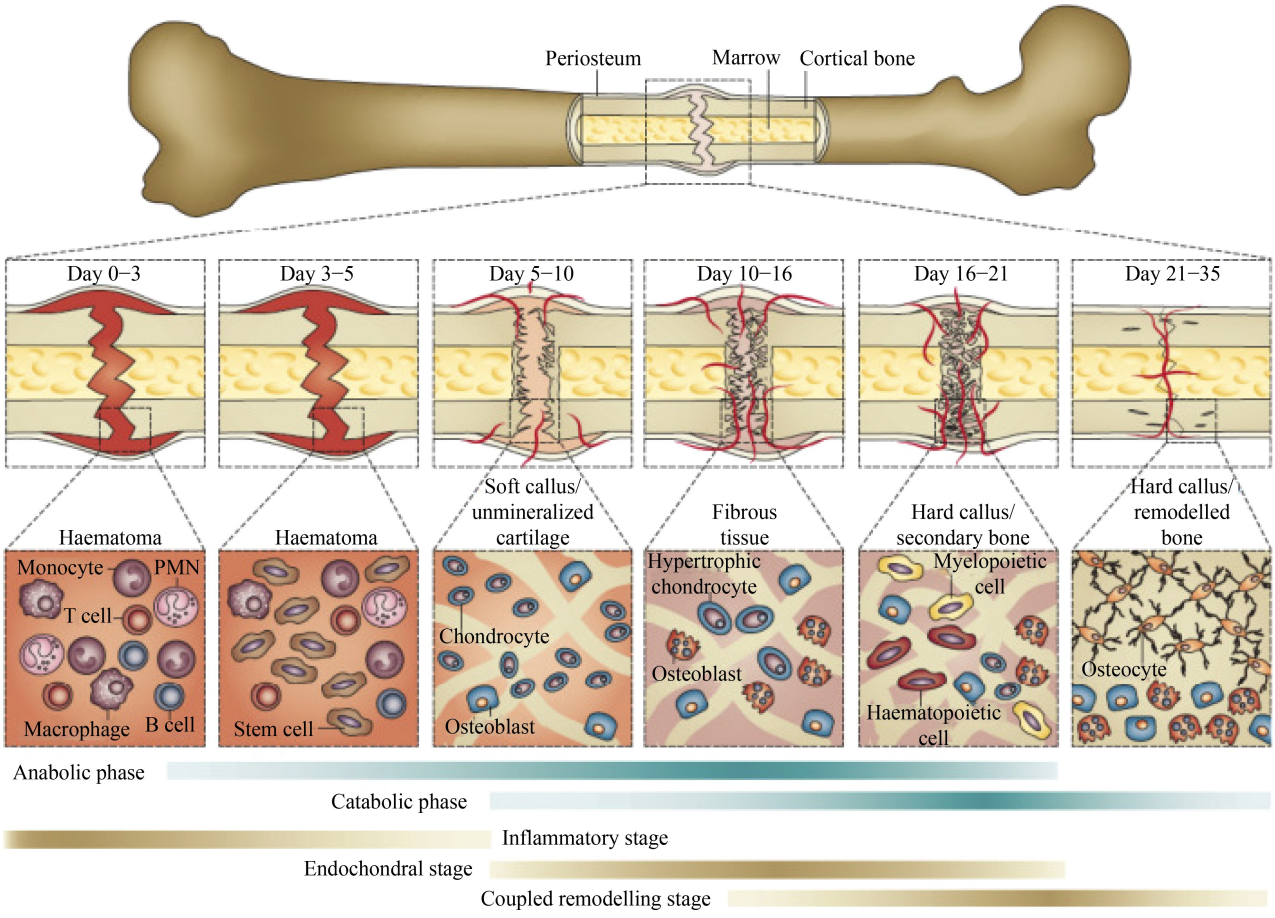

Fig. 4 Process of self-repair after bone fracture [14].

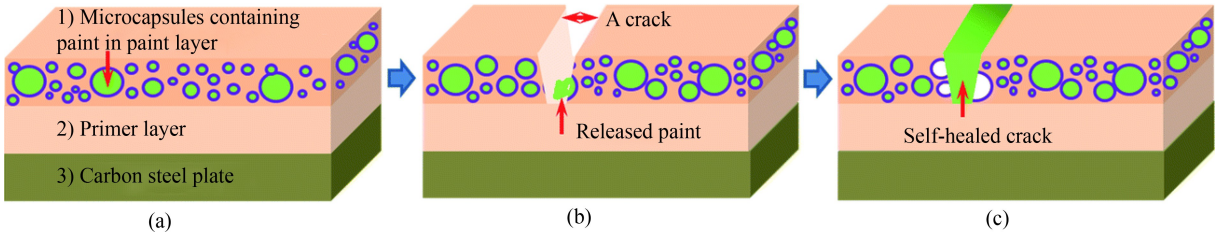

Fig. 5 Schematic of the microencapsulated self-repair process: (a) paint coating with microcapsules, (b) curing agent released to the layer, and (c) a crack healed by the agent [30].

structural properties [26]. The concept arises from the multi-functional vascular network in biological organisms and was initially developed in composite structures [27–29].

2.2.2 Intrinsic self-healing

Intrinsic self-healing materials introduce reversible bonds into the structural network. It heals mainly via dynamic covalent or non-covalent bond breakage and reorganization (Fig. 6). The topology of the cross-linked network can be changed by reversible exchange reactions and is called the dynamic covalent adaptive network (CAN) [31–33]. One of the mechanisms is dissociative exchange (Fig. 7(a)). The dynamic covalent bonds break into independent parts, which are active and can be restored under specific environmental conditions, such as light, heat, and catalysis. The density of the dynamic covalent network decreases. Bergman and Wudl [34] designed a self-healing material based on a thermally reversible Diels–Alder reaction. The other mechanism is associative exchange (Fig. 7(b)). Dynamic bonds tend to form chemical bonds with each other, which can also cause the other bonds to break. Montarnal et al. [35] used CAN in thermoset polymers and

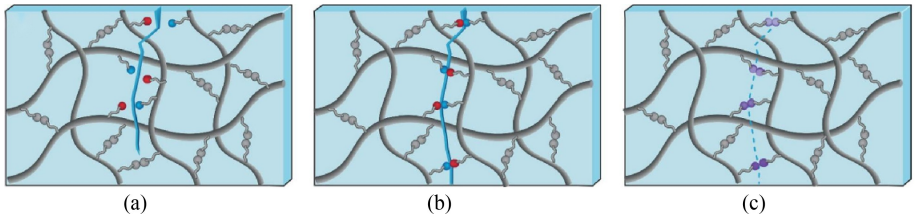

Fig. 6 (a) Dynamic bond breakage at the fracture surface, (b) dynamic bond reconnection after surface contact, and (c) final repair of the fracture surface [16].

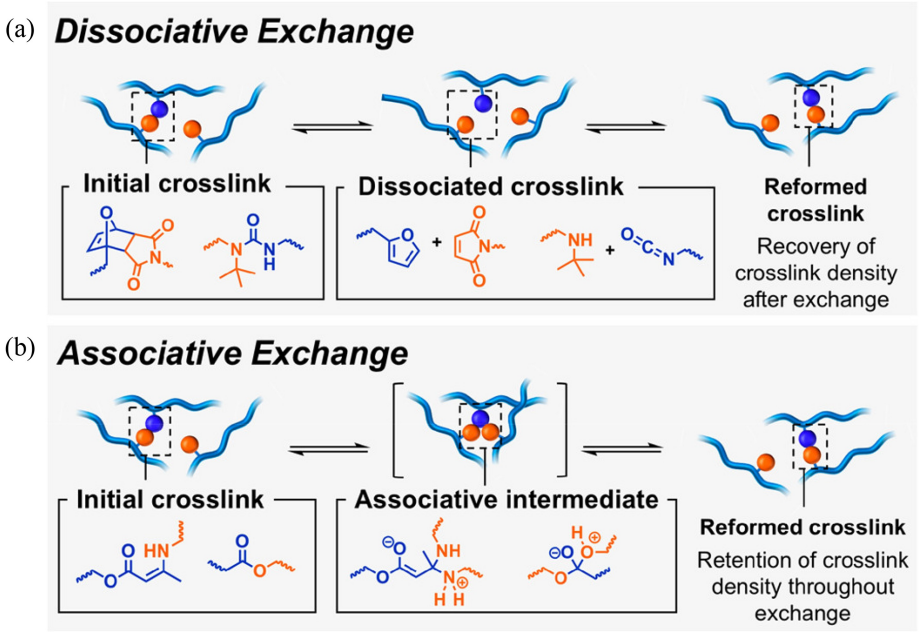

Fig. 7 Schematic of (a) dissociative exchange and (b) associative exchange [31].

transesterification at high temperatures to change the topology of the epoxy resin network. Exchange reactions are suppressed at ambient temperature, and the crosslinking density remains unchanged, resulting in good mechanical properties. It is believed to be the first polymer material to combine thermosetting and thermoplastic properties and to enable the self-healing of crosslinked resins. The rheological behavior of this polymeric material is similar to that of glassy silica, and such glass-like materials are referred to as a "vitrimer" [36–38]. Different vitrimers include reversible dynamic bonds such as ester bonds [39–47], disulfide bonds [48–56], diselenide bonds [57–60], and imine bonds [61–68].

In addition to chemical reactions, the topology of a network can be rearranged by reversible physical interactions, i.e., dynamic non-covalent bonds such as hydrogen bonds [69–72], coordinate bonds [73–76], and π–π stacking [77–79] in the structure of self-healing materials. It forms a combined and complex network and provides improved mechanical properties and healing efficiency.

2.2.3 Close-then-heal strategy

Another approach developed for self-healing involves a biomimetic close-then-heal (CTH) strategy. In the two-step healing category inspired by human skin, materials can repeatedly close macroscopic cracks at first, followed by extrinsic and/or intrinsic self-healing. The most critical pre-work is an external assistant that manually contacts the fracture surfaces before self-healing. A straightforward idea for this procedure is to utilize the shape memory effect as assistance. Materials with reversible plasticity can be fully recoverable upon heating, which is one of the normal ways to shape memory [80]. However, the ability to close cracks depends on the level of programming and the constraint during shape recovery. The effects of various design parameters (temperature and pre-strain) were shown on the crack closing efficiency with prior programming, laying a foundation for methods for designing CTH materials [81–83]. This healing form is expected to improve macrolength or structural damage; it is also considered a future trend in comprehensive healing.

3 Challenges for self-healing materials in various applications

Self-healing is popular in material science for specific types, such as polymer composites [84–89], coatings [90–96], cement [97–101], ceramics [102–104], organic dyes [105,106], concrete [18–20,107–109], and hydrogels [110–114]. Meanwhile, with the development of modern high-tech equipment in the direction of multi-functional integration, lightweight features, comfort, and intelligence, new challenges are posed to the structural design of self-healing materials, which require high stiffness and high damping performance under the action of a wide and dense frequency spectrum [115]. However, self-healing is often improved at the expense of improved mechanical properties. The stiffness and damping of materials are also contradictory. The development of self-healing materials in modern engineering applications revolves around the trade-off between these conflicting properties.

3.1 Conflict between mechanical and self-healing properties

The resin structure is a three-dimensional network formed by the physical or chemical crosslinking of polymer chains. Naturally, the chains are in a disordered state with high conformational entropy. However, after deformation caused by stretching, the structural order increases at different levels (Fig. 8), which decreases the overall conformational entropy. The mechanical energy from material deformation must be converted into molecular potential or thermal energy. Otherwise, the material breaks internally and creates new interfaces to dissipate the excess energy [116]. Structures with high stiffness and high damping then require strong crosslinks to resist the risk of potential damage from external forces. However, most of the dynamic bonds required for self-healing have a lower bond energy and preferentially break after deformation. In general, an excessive number of dynamic bonds weakens the mechanical properties, especially the stiffness, of the CAN.

3.2 Conflict between the stiffness and damping properties

Stiffness refers to the ability of a material or structure to resist elastic deformation when subjected to a force, whereas damping physically refers to the transformation or dissipation of energy via inelastic deformation. These methods are seemingly contradictory. For example, when a force is applied, a material structure with higher stiffness usually produces minor deformations with low levels of energy dissipation and poor damping performance. Thus, a performance index needs to be developed to describe the combination of stiffness and damping.

Let us take a quick review of the constitutive models for a viscoelastic material with damping capacity, aiming to identify a suitable evaluation index. First, consider an isotropic viscoelastic material under small deformation conditions. A generic one-dimensional stress–strain system can be given according to Boltzmann's superposition principle as follows:

$$\sigma(t) = \int_{-\infty}^{t} E(t-\tau)\frac{\partial \varepsilon(\tau)}{\partial \tau}\mathrm{d}\tau, \tag{2}$$

where $\sigma(t)$ and $\varepsilon(t)$ are the stress and strain component histories, respectively, and $E(t)$ represents the characteristic relaxation function in the time domain. For a standard linear solid, the dynamic

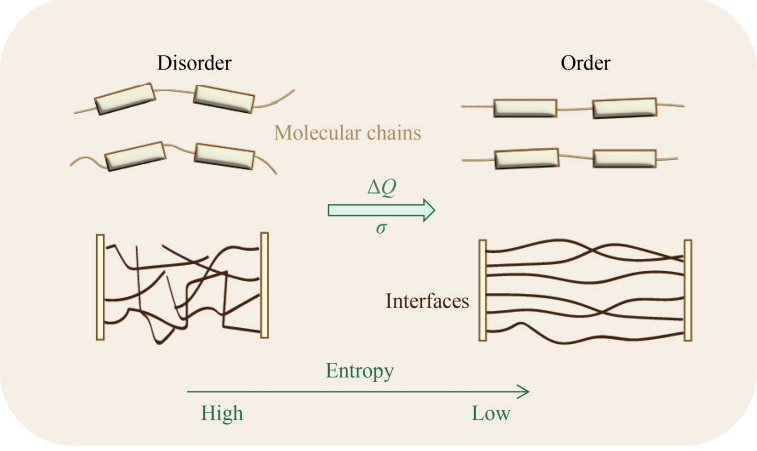

Fig. 8 Schematic of the microscopic conformation change in a polymer, where ΔQ denotes the dissipating energy, and σ denotes tensile stress.

function exhibits a relaxation that is exponential in time (i.e., the Zener model).

$$E(t) = E_0 + E_\infty \exp(-t/\tau), \tag{3}$$

where τ is the relaxation time, E_0 is the relaxed modulus, and E_∞ is the balance modulus. For polymers, however, the mechanical relaxation process may have more than one relaxation time. This relaxation behavior is widely characterized via the generalized Maxwell model.

$$E(t) = E_0 + \sum_{i=1}^{n} \delta E_i \exp(-t/\tau_i), \tag{4}$$

where δE_i is the relaxation contribution of each relaxation process. Furthermore, the relaxation time (Eq. (4)) eventually becomes a continuous spectrum because of the number of similar thermodynamic equilibrium states and multiple energy levels in the polymer network. This phenomenon leads to a case where $n \to \infty$ such that τ follows a certain distribution of $g(\tau)$. According to relaxation time distribution theory, the relaxation spectrum model can be written as

$$E(t) = E_0 + \delta E \int_0^\infty g(\tau) \exp(-t/\tau) \mathrm{d}\tau. \tag{5}$$

Considering the mechanical properties in dynamic tests, materials are subjected to steady-state oscillatory forcing conditions. Thus, the kernel function $E(t)$ in the different models can be converted by its Fourier transformation to the so-called complex modulus E^* as follows:

$$E^*(\mathrm{j}\omega) = E'(\omega) + \mathrm{j}E''(\omega), \tag{6}$$

where $E'(\omega)$ is the storage modulus, $E''(\omega)$ is the loss modulus, j is the imaginary sign, and ω denotes the angular frequency. The storage modulus characterizes the energy stored in a material due to elastic deformation and is often employed to represent the stiffness performance in dynamics. Additionally, $\tan\delta = E''(\omega)/E'(\omega)$ is defined as the loss factor, which characterizes the damping performance of materials. Other nomenclatures can be used to denote damping, such as the damping ratio, loss angle, log decrement, and quality factor. They can be transformed into each other in the case of low damping. Bert [117] reviewed various mathematical models and mechanisms of damping related to other mechanical properties. Here, $E''(\omega)$ is used as a figure of merit as the product of the modulus and loss factor, which often evaluates the combined performance of stiffness and damping as a guide for structural design.

Figure 9 shows the storage modulus and loss factor of common materials. The metal material occupies the upper left corner of the figure (i.e., high stiffness and low damping). In contrast, the elastic material occupies the lower right corner (i.e., low stiffness and high damping). The figure of merit for traditional materials is less than 0.6 GPa.

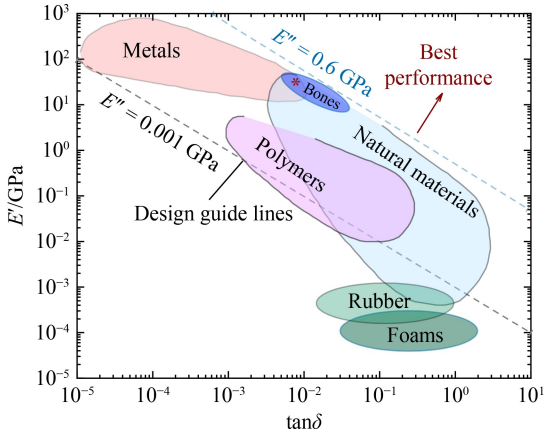

Fig. 9 Distribution of the storage modulus E' and loss factor $\tan\delta$ of engineering and biological materials at ambient temperature, data collected from Ashby [118].

Notably, as a structural material of animals, bone can reach a loss modulus of 0.6 GPa. It constructs its microstructure features at multiple levels, achieving a surpassing level of stiff yet lossy performance. As nature has inspired high-tech materials with self-healing properties, the design principle of multilevel structures can be learned from the unique bio-architecture of bones (Fig. 10). In engineering, the structural damping composites proposed in recent years combine the high damping properties of viscoelastic materials with the high strength and stiffness of structural materials [119]. Their damping is the hysteresis effect of component structures, which is caused by the stick–slip effect after the influx of many particles into the material structure, leading to irreversible dissipation via inelastic deformation. Inspired by structural damping materials (bones) in nature, stiff yet lossy properties can be further improved toward the best performance, as shown in Fig. 9, when the principle of structural design of composites is applied.

3.3 Relationships among self-healing, stiffness, and damping properties

The high self-healing performance of a material requires the introduction of many dynamic bonds, which tend to be more inclined to break when subjected to external forces, resulting in worse stiffness. At the same time, numerous dangling chains are introduced into the structure and crosslinked physically. It improves the dynamics and mobility of

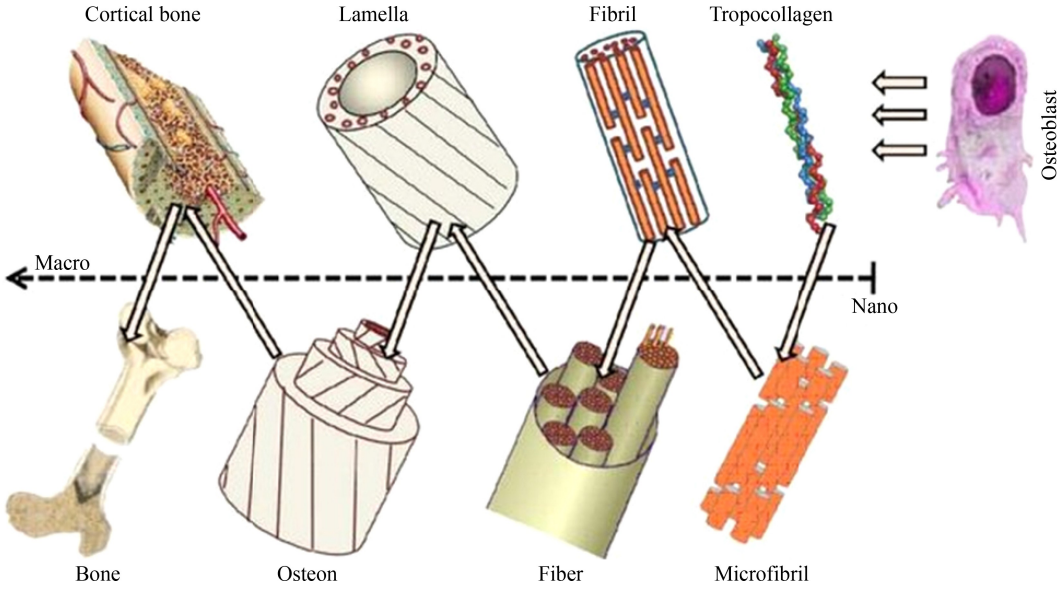

Fig. 10 Multiscale hierarchical structure of bone [120].

the chains, so the damping properties tend to be superior. A conceptual perspective of this triangular relation of self-healing, stiffness, and damping properties is shown in Fig. 11.

Presently, the predominant focus in the advancement of self-healing materials revolves around prioritizing the enhancement of recovery efficiency, followed by mechanical properties. The balance between the structural stiffness and damping properties has yet to be reported, which severely limits the controllable design and optimization of the comprehensive performance of self-healing composites. Here, we reviewed the current research on vitrimers, complemented by a limited but insightful exploration of a few structures in the context of stiffness and damping mechanisms. The recoverability of these materials is also included. Stiffness is characterized by the elastic modulus or the maximum storage modulus under dynamic conditions, and damping is evaluated by the peak loss factor $\max(\tan\delta)$ or the temperature range when $\tan\delta > 0.7 \cdot \max(\tan\delta)$.

4 Energy dissipation mechanisms at different levels

The effective damping performance of a damped composite structure relies not only on its intrinsic damping sources at the nanoscale but also on its extrinsic deformation-driving modes at the macroscale. Furthermore, the cross-scale coordination between intrinsic damping sources and extrinsic deformation-driven modes can originate from the microstructural architecture at noticeably different length scales from the microscale to the macroscale.

At the nanolevel, the intrinsic damping sources can

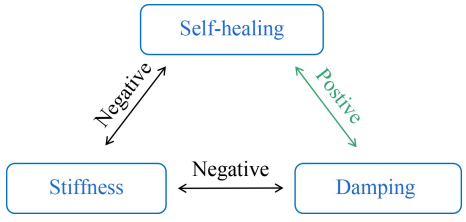

Fig. 11 Triangular relationships among self-healing, stiffness, and damping.

be divided into three main aspects: plastic damping, viscoelastic damping (physical crosslinks), and chemical damping. Plastic damping (Fig. 12(a)) refers to conventional material structures in which molecular chains are originally entangled, and after plastic deformation, when the structure is subjected to external excitation or vibration, the molecular chains undergo irreversible fracture and dissipate energy. Studies of hydrogels showed that chain fracture is the typical energy dissipation mechanism, and the classical Lake–Thomas theory prediction model for the intrinsic fracture toughness of elastomers can be used for chain fracture energy calculations [121–126]. Another mechanism is viscoelastic damping (Fig. 12(b)), in which the molecular chains in the structure can reform after a break. When mechanical energy is applied, this reversible physical connection breaks, forming many dangling chains that undergo slip, entanglement, and diffusion, i.e., internal friction between molecular chains. The different physical crosslinking points can subsequently automatically lap to restore an equilibrium state, thus dissipating the mechanical energy. Notably, physical crosslinking is achieved by introducing dangling chains and reversible non-

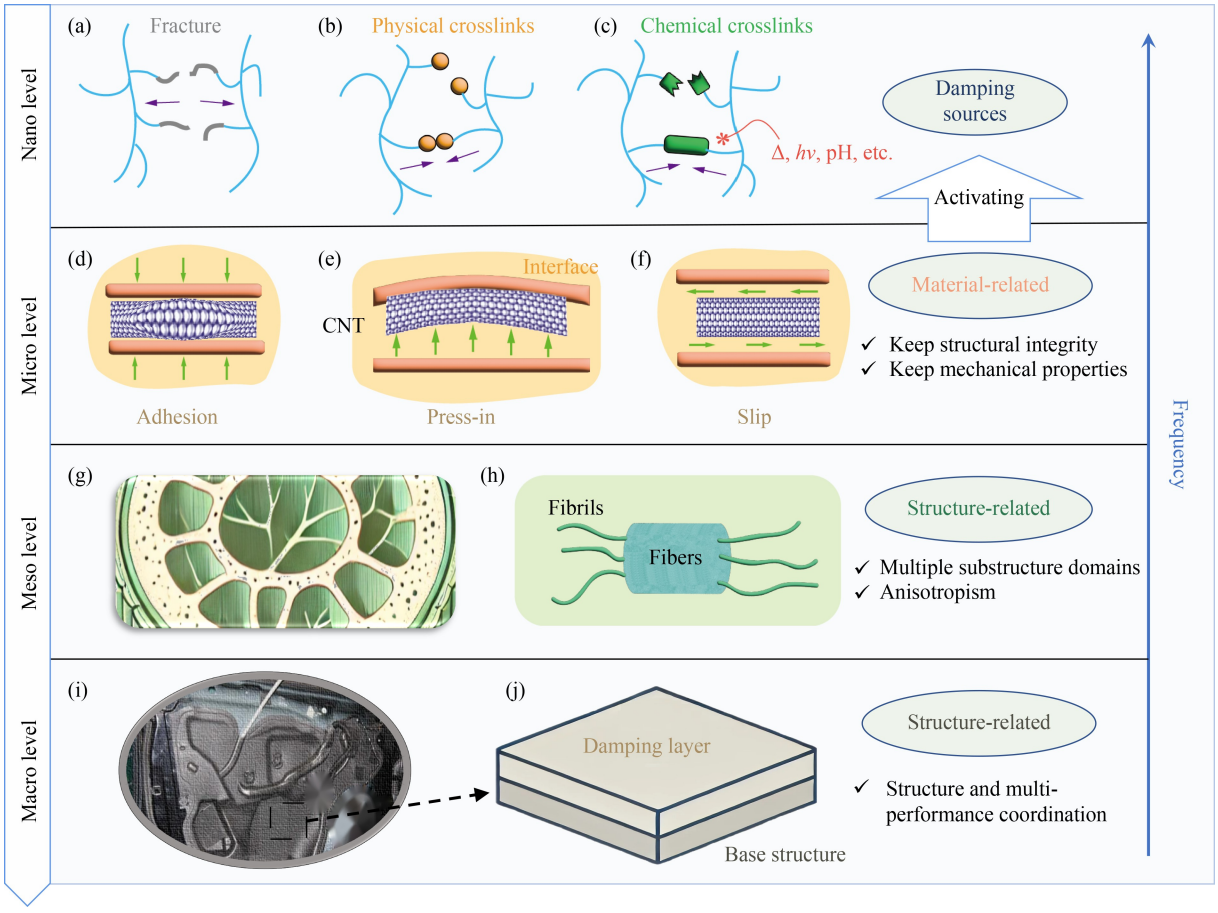

Fig. 12 Dissipation mechanisms at different levels. (a) Plastic damping, (b) physical damping, and (c) chemical damping refer to the damping sources at the nanolevel. Interfacial interactions, including (d) adhesion, (e) press-in, and (f) slip effects, refer to interfacial damping at the microlevel. Interactions between substructure structure-level designs, such as (g) cellular structures and (h) fiber reinforcement at the mesolevel. A practical application of macrostructural design on the (i) cab door, with (j) free damping layers laid over it.

covalent bonds to achieve automatic scission and formation. However, for self-healing vitrimers based on reversible covalent chemical bonds, a new intrinsic damping source arises: the chemical damping mechanism (Fig. 12(c)). It differs from plastic damping in that the particles are connected by dynamic chemical bonds, and its scission and formation process is reversible; however, the difference with viscoelastic damping is that the reversible reaction requires agitation from various environments, such as temperature, light, and ionic strength.

At larger scales, the interfacial interaction plays a crucial role. As shown in Figs. 12(d)–12(f), the filler at the microlevel (carbon nanotube [CNT]) can introduce more interfaces, accompanied by the scission and reformation of physically crosslinked chains in the network. Although there are internal forces between the interfaces, the equilibrium state can be reached by mutual complementation, interaction, and consistency. The strain generated here is elastic. However, when external forces cause additional inelastic strains, the system is in a non-equilibrium state. The stress jump occurs at the interface due to the different elastic moduli between the filler and matrix. Thus, a "driving force" for relaxation is generated, which can lead to adhesion, slip, and press-in effects between the interfaces, thus providing sufficient interfacial damping to increase dissipation. A variety of characteristic substructures can be constructed at the level of mesostructural design, such as cellular structures and artificial fiber composite structures (Figs. 12(g) and 12(h)). The neighboring substructures are close to the degenerate energy state. When excited by a load, the energy barriers can be overcome by strain energy between the degenerate energy levels, and the jumping effect can enhance the dissipation performance. The design of a specific structure at the macrolevel, followed by the design of a specific damping composite structure (Figs. 12(i) and 12(j)), is the key to cascading the excitation of dissipation at each scale.

Table 1 shows the differences across length scales.

Table 1 Differences in the individual scales of hierarchical structures

Scale	Spatial characteristics	Mechanisms	Applications
Nanoscale	Discrete	Plastic, physical, and chemical damping (damping sources)	Self-healing polymers
Microscale	Discrete-continuous	Adhesion, press-in, and slip effects (damping excitation)	Nanocomposites
Mesoscale	Continuous	Adhesion, press-in, and slip effects (damping excitation)	Structural materials
Macroscale	Continuous	Adhesion, press-in, and slip effects (damping excitation)	Structural systems

Plastic damping, viscoelastic damping, and chemical damping at the molecular level correspond to the mechanisms of damping generation at high frequencies and the sources of energy dissipation at the smallest scale. The incorporation of fillers at the microlevel is characterized by interfacial interactions that stimulate dissipation without sacrificing mechanical properties or structural integrity [127,128]. Interfaces are also important for mesoscale substructures composed of different material components, which can combat the premature failure of composites and increase energy dissipation by deflecting cracks. The main difference is that structural integrity is not guaranteed and tends to interact between substructures, resulting in anisotropy. The macroscopic structural design is concerned with the objective multi-performance requirements and damping structures to maximize the excitation of the dissipation properties of the damping material at all levels under deformation. The dissipation mechanisms of each level are discussed in detail in the following subsections.

4.1 Chain scission and formation at the nanoscale

The origin of energy dissipation of a material at the molecular level can be stated in terms of the characteristics of the material itself. The stress–strain curve of an inelastic material is shown in Fig. 13. It

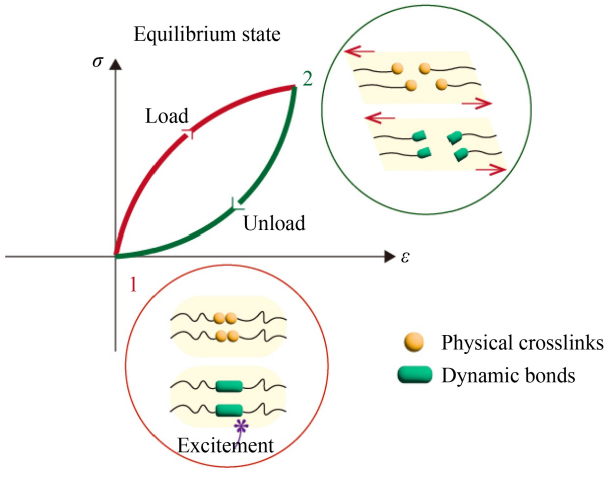

Fig. 13 Hysteresis loop caused by inelastic deformation at equilibrium and schematic of the state of chain scission and formation.

deviates significantly from the ideal elastomer at the working stress, and the strain characteristic is called hysteresis. Here, crosslinks and dynamic bonds are broken after loading but reformed after unloading, remaining at equilibrium. However, during a dynamic load, the stress–strain curve forms a loop (Fig. 14(a)), while the material is at non-equilibrium, and the mechanical hysteresis indicates the energy absorbed during the loading and unloading cycles. The area enclosed by a hysteresis loop represents the exact amount of energy dissipation ΔQ per unit volume of material in one cycle, that is,

$$\Delta Q = \oint \sigma(t)\mathrm{d}\varepsilon(t) = \oint \sigma(t)\frac{\partial \varepsilon(t)}{\partial t}\mathrm{d}t. \tag{7}$$

In polymers, chain segment motion during the glass transition requires overcoming internal friction, which essentially involves the scission and reformation of physical crosslinks at the nanolevel. For self-healing networks containing dynamic bonds, the heterogeneity of motion units increases, and it reaches a higher level of diversity, resulting in additional relaxation components. Thus, Eq. (2) can be rewritten for chemical damping as follows:

$$\sigma(t) = \int_{-\infty}^{t} \left[E_{\mathrm{phy}}(t-\tau) + E_{\mathrm{che}}(t-\tau)\right] \frac{\partial \varepsilon(\tau)}{\partial \tau}\mathrm{d}\tau, \tag{8}$$

where E_{phy} and E_{che} denote the relaxation functions for viscoelasticity of the polymer itself and chemical reactions of the dynamic bonds, respectively. Relaxation is exactly dependent on the temperature. The temperature dependence of the relaxation time follows the Arrhenius equation:

$$\frac{\tau}{\tau_0} = \exp\left[\frac{E_a}{R}\left(\frac{1}{T} - \frac{1}{T_0}\right)\right], \tag{9}$$

where E_a is the activation energy of relaxation, R is the gas constant, τ_0 is the reference relaxation time, and T_0 is the reference temperature in Kelvin. Another relationship between the relaxation time and temperature is given by the WLF equation, which is only applicable above the glass transition temperature.

$$\log\left(\frac{\tau}{\tau_0}\right) = \frac{C_1\,(T - T_0)}{C_2 + (T - T_0)}, \tag{10}$$

where C_1 and C_2 are the parameters. At each

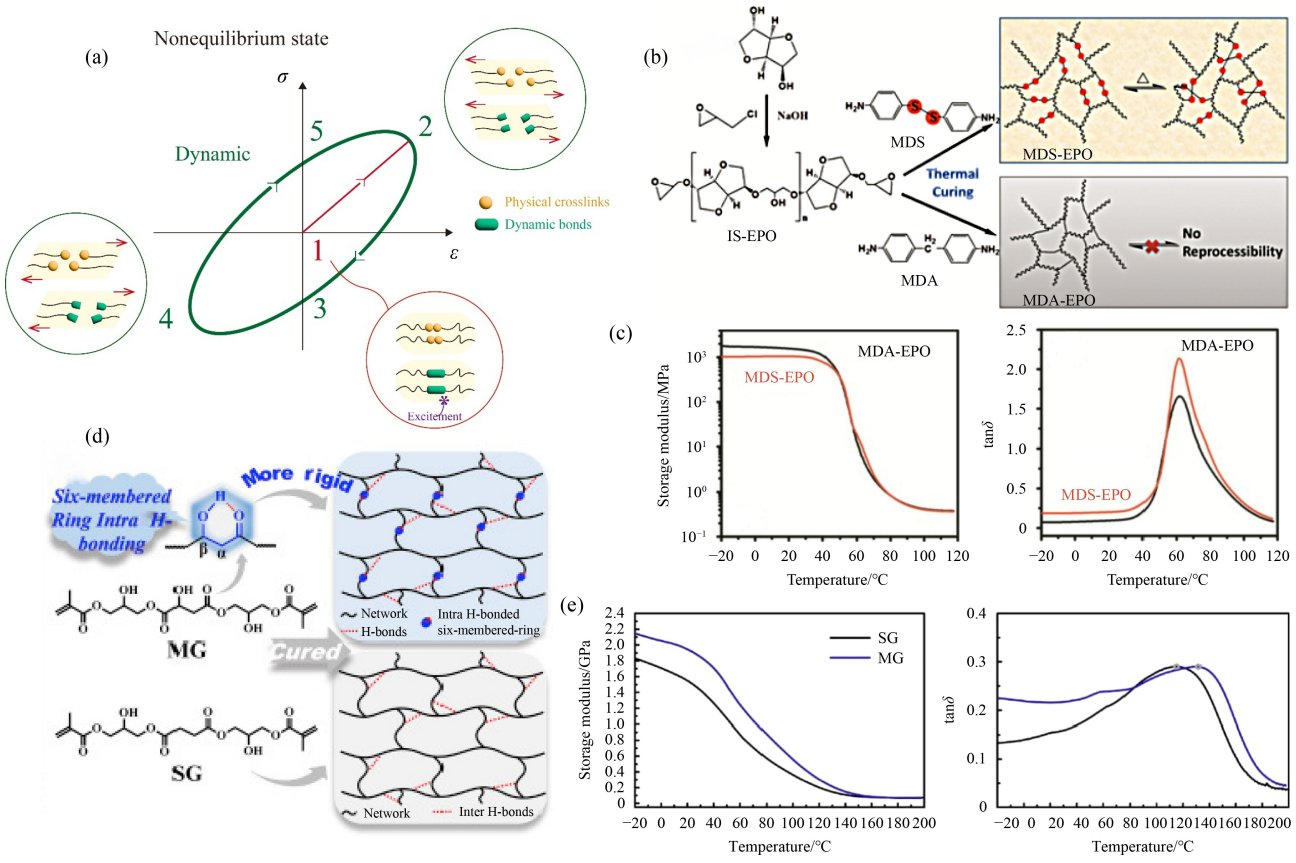

Fig. 14 (a) Hysteresis loop caused by inelastic deformation at non-equilibrium and schematics of the step-by-step breakage and connection of physical crosslinks and chemical bonds at non-equilibrium. (b) Schematic of the chemical structures of MDS with disulfide bonds and MDA without dynamic bonds and (c) comparison of the material properties [53]. (d) Schematic of the chemical structure of the self-healing material MG, which contains more hydrogen bonds than the other material SG, and (e) comparison of the material properties [129].

temperature, the angular frequency ω of relaxational motion is equal to that of the dynamic force. This variable can be expressed as the inverse of the relaxation time as follows:

$$\omega\tau = 1. \tag{11}$$

These expressions are related to time and frequency with respect to the dynamic viscoelastic properties of a polymer, known as time–temperature superposition.

In self-healing polymers, the extra relaxation behavior is induced by dynamic bonds, which can be described by the same kernel function as the polymer viscoelastic relaxation function (Eq. (3)). Its temperature dependence also follows the Arrhenius relationship. More descriptively, self-healing dynamic bonds result in a greater variety of chain scissions and formations, increasing the diversity of relaxation motions, which also results in additional chemical damping. The abovementioned expressions suggest that the coupling of viscoelastic relaxation (physical damping) and exchange reactions (chemical damping) not only increases the peak value of the loss but also broadens the damping effective temperature (or frequency) range. As shown in Figs. 14(b) and 14(c), epoxy resins containing disulfide bonds and self-healing functions (MDS-EPO) possess higher loss factors and wider damping temperature ranges than epoxy resins without dynamic bonds (MDA-EPO). Increasing the number of implanted intramolecular hydrogen bonds in a self-healing polymer network has obvious advantages in terms of stiffness and damping (Figs. 14(d) and 14(e)).

4.1.1 Chemical damping via dynamic covalent exchange

Berne et al. [40] designed a self-healing polymer based on transesterification exchange with a recovery rate of 87%. The prepared epoxy resin based on the di-glycidyl ether of bisphenol A (DGEBA) possessed a wider damping temperature range after self-healing, increasing the peak loss factor from 0.7 to 1.0. Conversely, its modulus decreased, confirming the relationship between stiffness and damping. Lu et al. [41] prepared a self-healing epoxy resin using phthalic anhydride as a hardener with an elastic modulus of

1.8 GPa, a loss factor exceeding 0.6, and a self-healing efficiency of up to 88.1%. Xu et al. [42] reported that as the mint diamine (MDA) content in a polymer increases, the number of active amino hydrogen atoms it also contains increases rapidly. Hydrogen can form reversible bonds with the epoxy group of tung oil-based tri-glycidyl ester (TOTGE), increasing the internal consumption of the structure and improving the healing efficiency, resulting in an increase in the loss factor from 0.78 to 0.95. Azcune et al. [49] prepared self-healing epoxy resins based on rigid DGEBA and flexible di-glycidyl ether of poly (propylene glycol). The peak loss factor of the polymers increased from 0.97 to 1.62 with increasing content of the flexible structure, which promoted the viscous flow of the chain. The imine exchange, also known as the Schiff reaction, consists of two processes: polymerization, hydrolysis, and exchange [130]. Therefore, imines also have the potential to establish DCANs. Rashid et al. [61] prepared two epoxy resins containing imine bonds via two aldehydes (VAN and SYR) and bis-aminomethyl cyclohexane (BAC) with a recovery efficiency close to 100%. Given the rigid structure contained in their components and the non-coplanar structure of BAC, which increases the friction between the molecular chains, materials with a high loss modulus close to 0.4 GPa and a storage modulus of approximately 3 GPa were obtained.

Most polymers rely on the introduction of "soft matter" with reversible bonds for their healing properties, whereas the stiffness depends more strongly on the matrix structure. However, the rigidity and flexibility of each component are different, which can effectively broaden the glass transition temperature range and damping properties of the polymer. Yu et al. [63] prepared an epoxy with dynamic imine covalent exchange by curing the structure of vanillin (Van-Ep) with isophorone diamine (IPDA). The loss factor peak domain of Van-Ep is wider because of the greater stiffness of vanillin. The difference in molecular motility promotes the mutual hysteresis effect between the components (Fig. 15), reaching a maximum loss factor of 1.8 and a healing efficiency of 100%. In addition, Denissen et al. [64] improved the dissipative capacity of the prepared materials by polymerizing cyclohexane dimethanol bis-acetoacetate with amine, resulting in a fast reversible reaction, short relaxation time, and high density of dynamic bonds. The materials possess a storage modulus of 2.4 GPa and a loss factor of approximately 1.25 and restore 100% of their mechanical performance after several remodeling cycles. Huang et al. [131] prepared self-healing epoxy resins with a homogeneous sea-island structure using polyethylene wax and epoxy resin blends. They used the crosslinked structure of the epoxy resin as the continuous phase and the polyethylene wax as the dispersed phase and were also able to achieve a high loss factor of 1.1.

4.1.2 Physical damping via physical non-covalent exchange

Viscoelastic damping occurs in nearly all of the polymers. However, there is a special physical connection called dynamic non-covalent bonding. For example, hydrogen bonding interactions are common intermolecular forces in self-healing polymers. Molecular structures can self-repair damage due to the recombination of hydrogen bonds (Fig. 16). The energy of a single hydrogen bond is weak, and most self-healing polymers based on hydrogen bonding have been studied for elastomers and flexible electronics [88,89,132–134]. However, the juxtaposition of duplex, triplex, and quadruplex hydrogen bonds can quickly form a reversible hydrogen bonding network structure, substantially improving the mechanical properties of the structure. Guadagno et al. [135] functionalized multi-walled CNTs (MWCNTs) with

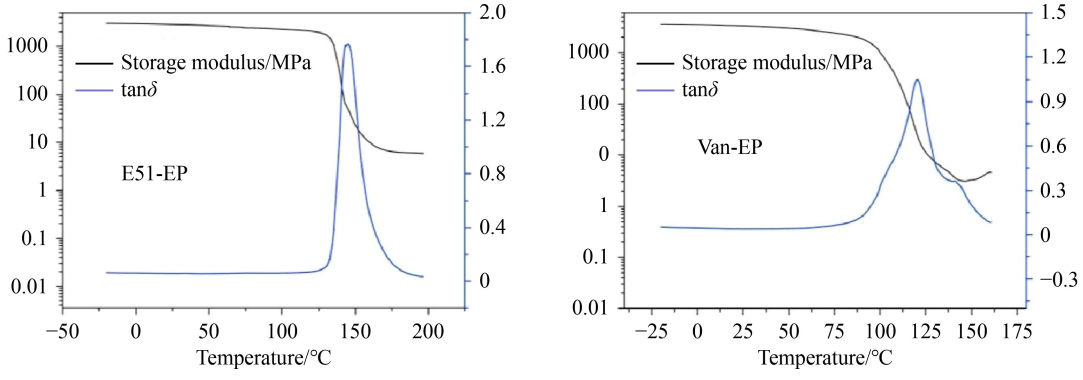

Fig. 15 Comparison of the mechanical properties of Van-EP and E51-EP, where E51-EP is the control group without dynamic bonds [63].

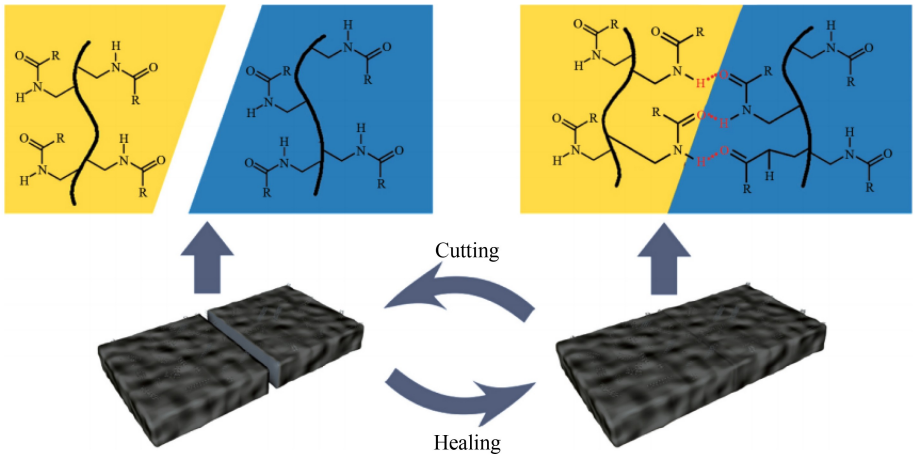

Fig. 16 Cutting and healing process of reversible hydrogen bonds [136].

thymine and barbituric acid, which can be covalently bonded to CNT walls as hydrogen bond donors and acceptors, providing dynamically exchangeable functionality and allowing better packing dispersion. Then, a hydrogen bonding supramolecular network is formed. When subjected to external forces, the hydrogen network is disrupted, reformed, and absorbs a large amount of energy, leading to increased molecular chain motion. Materials with different CNT contents have excellent mechanical properties, with energy storage moduli between 2 and 3 GPa at room temperature and loss factors close to 0.6, but the self-healing efficiency ranges from 50% to 54%.

In addition, two or more non-covalent bonds of different strengths have been introduced into polymers. The weaker non-covalent bonds impart energy-dissipating properties, and the stronger non-covalent bonds enhance the material's mechanical properties. For example, metal coordination bonds are special non-covalent bonds widely considered among the most robust supramolecular interactions. Metal coordination occurs mainly by self-assembly, with the metal at the apex linked by rigid or semi-rigid organic ligands. It is much stronger than other non-covalent interactions and is reversible, thus compensating for the disadvantages of reversible covalent and non-covalent bonds [137]. Metal–ligand bonds are often used to construct self-healing elastomers. Wang et al. [138] introduced the coordination interaction of diamide pyridine and Fe^{3+} into polyurethane and obtained self-healing polyurethanes with up to 100% self-healing efficiency. In addition, Burattini et al. [77] combined hydrogen bonding and π–π stacking mechanisms to achieve self-repair of polyurethanes. A hydrogen-bonded supramolecular network was introduced to form a hybrid copolymer system with a recovery rate of more than 95%. The damping of the supramolecular structure is due to the influence of the two superimposed networks, which results in good performance, with the loss factor reaching 0.5 in the low-frequency region.

4.1.3 Plastic damping via chain fracture

The plastic damping mechanism requires that the molecular chains in the process zone can be fractured effectively. In practice, many molecular chains of relatively short length are usually introduced into the polymer structure to promote fracture [139–141]. When the structure is deformed, the short chains can be irreversibly ruptured (Fig. 17(a)) to dissipate mechanical energy. Figure 17(b) shows the stress–strain curves of plastic materials at equilibrium. The strain after unloading is due to the irreversible fracture of chains.

4.2 Interaction of interfaces with the matrix at the microscale

At the microscale, a composite material with a surpassing interface, which provides abundant extrinsic deformation-driving modes, is the key to improving damping performance. It can combine the stiffness and damping properties of the matrix and filler, and the filler–filler and filler–matrix interactions can increase the hysteresis and internal dissipation of the structure, thus enhancing the damping properties. High-performance and controllable interfaces can be obtained by selecting zero-dimensional (e.g., nanospheres [142–144] and diamond nanoparticles [145–147]), one-dimensional (e.g., CNTs [148–150] and boron nitride nanotubes [151–153]), and two-dimensional (e.g., graphene [154–156], graphene oxide [157,158], and clay nanosheets [159]) nanomaterials with lightweight, high-strength, and high-stiffness characteristics as nanofillers for composite materials. The matrix and the filler and its surface constitute several interfacial layers (Fig. 18). The interfacial

interactions can be attributed to entanglement, chemical bonding, electrostatic adsorption, and mechanical self-locking, which add great entropic forces to the structure and effectively transfer the stress from the matrix to the stiffer filler.

Figure 19(a) is presented to provide an intuitive explanation. Interfacial damping includes covalent bonds, van der Waals (vdW) interactions, and interlocking between the filler (e.g., CNTs) and the matrix, which play a major role [163], while the

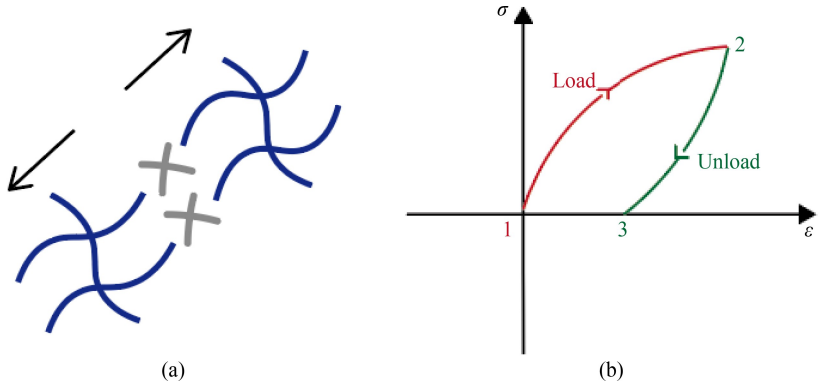

Fig. 17 (a) Schematic of irreversible breaks between molecular chains. (b) Hysteresis loop caused by plastic deformation.

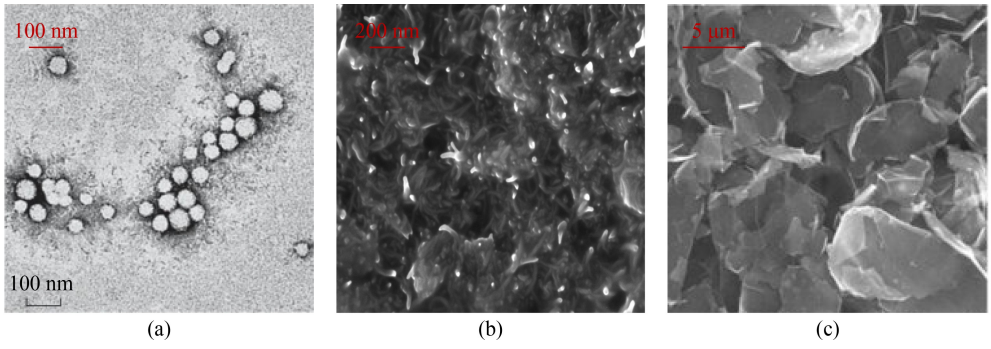

Fig. 18 SEM images of the interface with (a) nanoparticles, (b) CNTs, and (c) graphene [160–162].

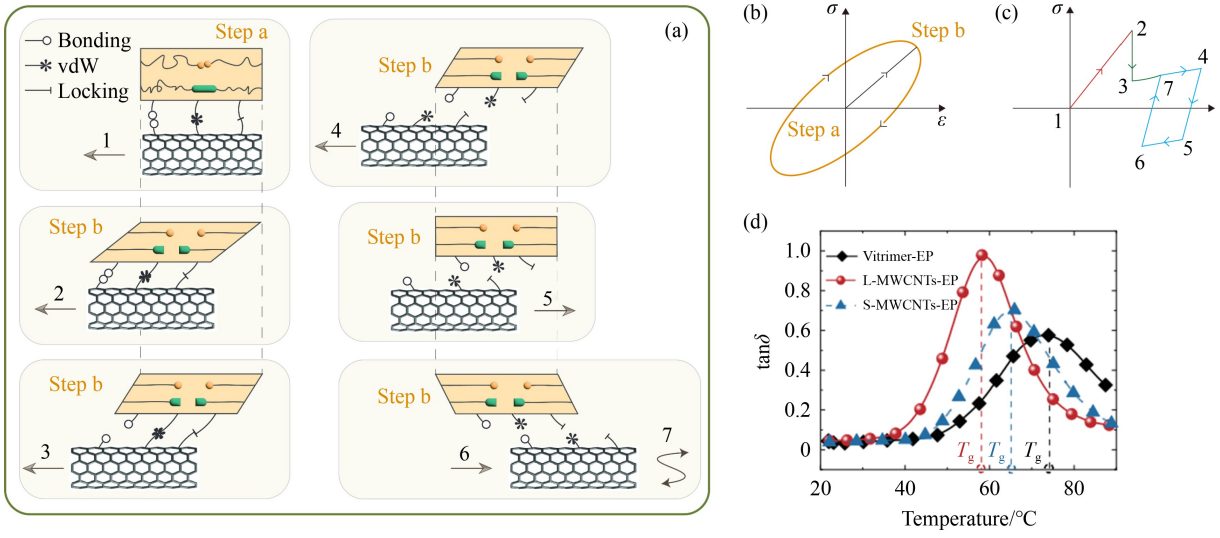

Fig. 19 (a) Schematic representation of damping from the interface and matrix during loading. (b)(c) stress–strain curves of the corresponding steps. (d) Temperature-dependent diagram of the loss factors of the vitrimer matrix (black curve), the vitrimer with long MWCNTs (red curve), and the vitrimer with short MWCNTs (blue curve) [5]. vdW: van der Waals force.

viscoelasticity of the matrix also contributes to energy dissipation. After the dynamic loading is applied and the critical stress is reached (2 and 3 in Fig. 19(a)), the interface debonds with irreversible disruption of covalent bonds, leading to sliding and dissipation. Then, the physical interactions continue to break, and the energy dissipates with the slip at the interface (3 and 4 in Fig. 19(a)). When the load is reversed and cycled back and forth, the dissipation process is similar (4–7 in Fig. 19(a)). During the process, vdW and interlocking are disrupted, leading to inelastic deformation of the viscoelastic matrix along with the breakage and formation of molecular chains at the nanolevel, and viscoelastic damping or even chemical damping is excited. This characteristic is also shown in the stress–strain curves in Figs. 19(b) and 19(c). Energy dissipation at the microscopic level couples the interfacial damping and viscoelastic damping of the matrix, which involves a damping mechanism at a smaller scale. The effects of different MWCNTs on the mechanical properties of self-healing materials were studied (Fig. 19(d)), and the loss factor of the self-healing epoxy resin was significantly improved by the introduction of nanofillers.

4.2.1 Nanoparticles

Common nanoparticles include TiO_2, SiO_2, $CaCO_3$, and montmorillonite. Liu et al. [43] prepared an epoxy based on β-hydroxy ester bonds with functionalized silica reinforcement called Esilica (Fig. 20). Given the multiple reactive sites on the Esilica surface, there might be molecular chains attached to the surface. The contact area between the nanoparticles and the matrix is relatively small, leading to a weak interface effect. The mobility of those attached chains is reduced, and it is extremely difficult for them to participate in relaxation. Therefore, a higher crosslinking density leads to greater stiffness, whereas a longer relaxation time results in a lower peak loss factor but a wider effective loss range. Barabanova et al. [164] tested a self-healing silica composite and demonstrated a similar effect of nanoparticles on the mechanical properties of the composite (Fig. 20(b)). Furthermore, a vitrimer with thiol group-functionalized silica with a high modulus of 2 GPa and a high healing efficiency of 80% was tested, but the loss factor was only approximately 0.5 [54].

4.2.2 CNTs

CNTs possess excellent mechanical properties. It can absorb many molecular chains and connect them to the matrix to form an effective interfacial region. However, CNTs are highly prone to aggregation, leading to stress concentration and a decrease in structural properties. One of the critical issues to be addressed when incorporating CNTs into polymers is to improve their dispersion to achieve good interfacial properties and improve their structural and damping properties. Zhou et al. [50] designed an epoxy resin based on disulfide. They introduced polypyrrole-modified MWCNTs, which were more uniformly dispersed in the polymer network, to obtain a storage modulus of 2.2 GPa and a maximum loss factor of approximately 0.9. Yang et al. [39] used polymers with intrinsic microporosity to enable better dispersion of MWCNTs in self-healing epoxy resin, which increased the elastic modulus of the material to 1.7 GPa, with a maximum loss factor of approximately 1.75. Meanwhile, the photothermal properties of the CNTs can catalyze the healing reaction, with an efficiency of 80%. Xu et al. [11] prepared a surpassing damping and modulus nanocomposite with CNTs based on a self-healing epoxy and established a damping model to recognize the relaxation time spectrum of the composite. In

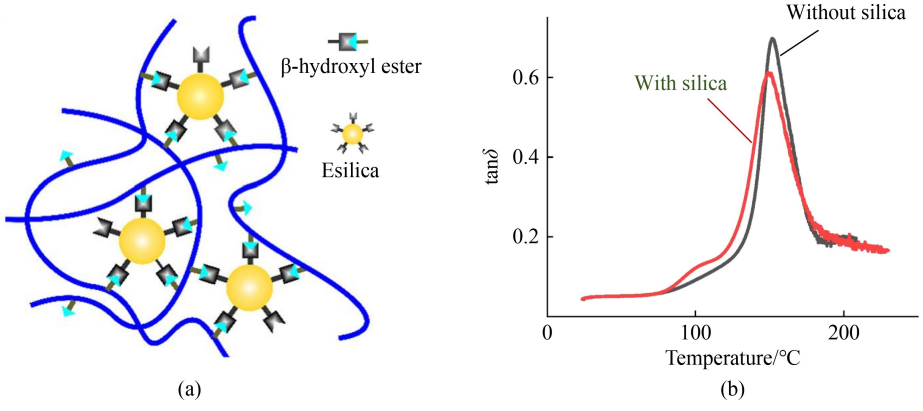

Fig. 20 (a) Schematic of a silica-enhanced network structure and some welded joints on the silica surface [43]. (b) Comparison of loss factors before and after the addition of silica nanoparticles to a vitrimer [164].

addition to the high modulus and high loss factor, the damping peak is also characterized by a considerable width, leading to a substantial increase in the effective frequency range (Fig. 21).

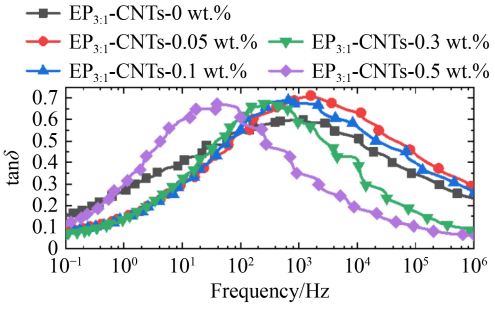

Fig. 21 Frequency-dependent loss factors of self-healing epoxy (shown as $EP_{3:1}$ in the figure) with different contents of CNTs [11].

4.2.3 Graphene

Graphene is a typical two-dimensional nanofiller with extremely high physical strength and is the thinnest and most rigid material in the world. Graphene has a vast surface area and high elastic modulus and is nearly equal to a rigid body within the polymer matrix. Thus, the intact interface formed would mainly bear the tensile load on the polymer, and interfacial adhesion becomes the predominant mechanism for graphene reinforcement [165]. Katsiropoulos et al. [166] reported that the loss modulus and loss factor increased considerably with increasing graphene nanoplatelet content and that the frequency dependence was negligible. Yang et al. [45] developed a shape-memory graphene/vitrimer. The graphene surface is rough, and its frictional dissipation and microcrack extension resistance are more pronounced than those of smooth-surface pure epoxy. Moreover, its good dispersion and lubricity help load transfer from the polymer to graphene, promoting more significant deformation and shape reconfiguration. A modulus of approximately 2 GPa, a high loss factor near 2.0, and a healing efficiency close to 100% were achieved. Li et al. [167] also explored the synergistic effect of graphene and CNTs in a self-healing polyurethane. As more CNTs are incorporated, they form a spatial structure and optimize the interface properties. The stresses are distributed along the direction of the interface between the filler and the matrix, which even creates mechanical interlocking and improves the dissipating capacity.

4.3 Construction of structural features at the mesoscale

When a high-damping material does not undergo mechanical deformation, no mechanical energy is stored, and no energy dissipation occurs. The mesoscale unit is a feature structure with a certain spatial arrangement of damping elements formed by a specific artificial design, aiming at applying vibration excitation to the damping elements via the feature structure to realize the damping excitation effect. The main damping mechanism of structure-damped composites with mesoscale feature structures is still interactions at the interface, but the difference from that of nanocomposites is that the structural integrity of the material is not guaranteed but tends to be anisotropic.

4.3.1 Natural biological features

Hierarchical structural designs at the mesolevel can present larger microstructural features. The natural structure of bio-materials has been developed over millions of years; therefore, researchers always learn first from nature, e.g., the bones mentioned earlier in this paper. In addition, the structures of nacre, crab, and bamboo have excellent mechanical properties and a fine hierarchical design (Figs. 22(a)–22(c)). This phenomenon inspires the design of artificial composites. Self-similar bio-materials exhibit repeating geometrical patterns at different scales [168,169] (Fig. 22(d)). This inherent characteristic enables the effective distribution of mechanical loads and enhances energy dissipation. The scale-invariant properties provide excellent damping performance, especially under dynamic and impact-loading conditions, as they can absorb vibrations efficiently across a wide range of frequencies. Gradient bio-materials feature spatially varying properties, such as stiffness, density, and porosity, across their volume [170,171]. In the gradient structure of pinecones, the porosity is distributed in a gradient from inside to outside (Fig. 22(e)). Moisture exposure leads to a strain gradient across the scale, which is helpful for reversibly opening and closing to disperse seeds. Therefore, gradient structures allow for smoother transitions in stress and strain, which can significantly improve vibration damping and reduce resonance effects. The gradual change in mechanical properties helps mitigate sharp stress concentrations, enhancing material performance in vibration-critical applications [172]. Additional bio-inspired features, such as porous structures (e.g., coral and sponges) or hierarchical architectures (e.g., wood or bamboo), also further contribute to the energy dissipation properties.

4.3.2 Particle- and fiber-reinforced composites

Micron-sized particle composites incorporating

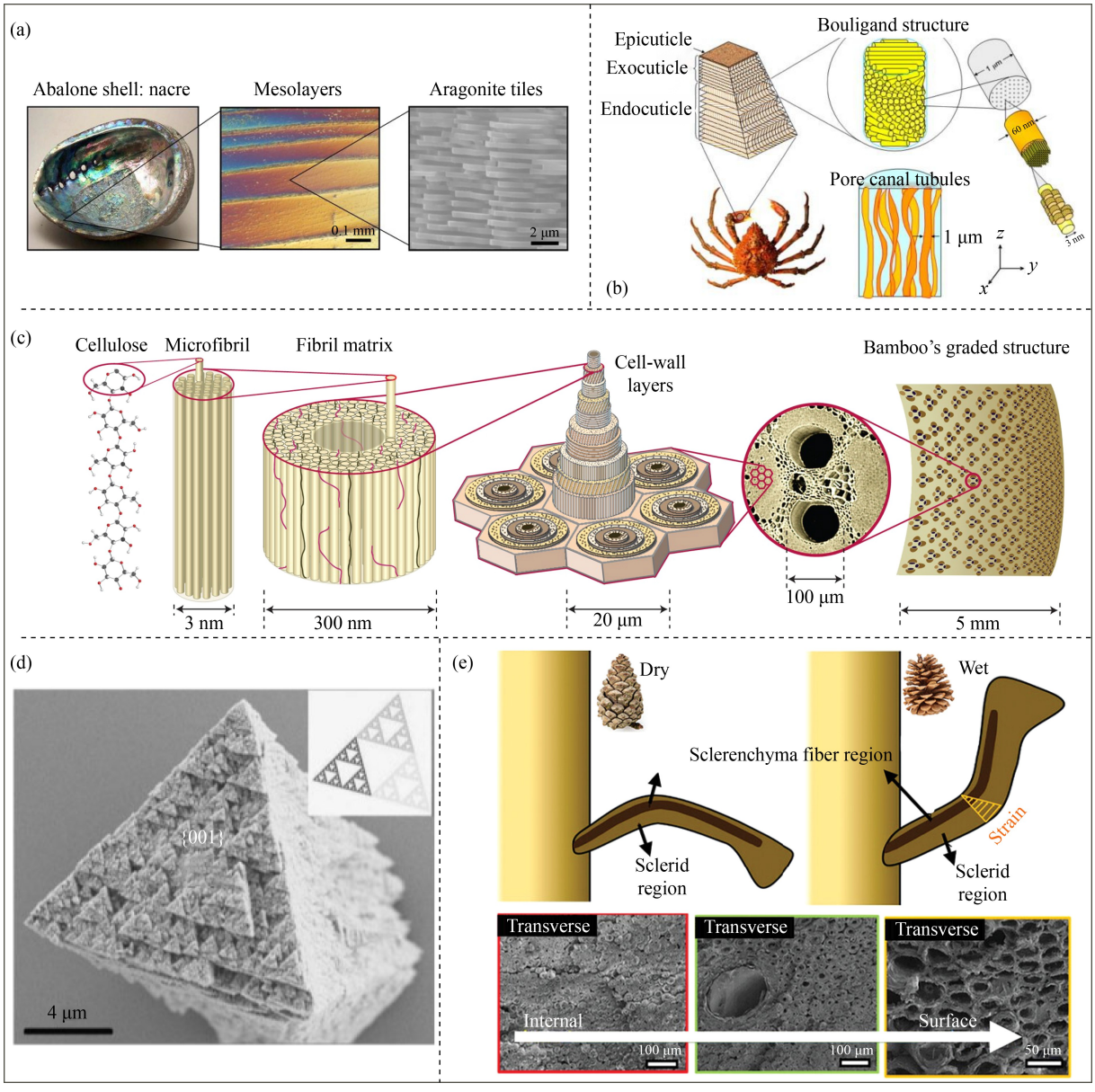

Fig. 22 Schematics of the natural hierarchical structures of (a) nacre [173], (b) crab carapace [174], and (c) bamboo [175]. (d) Image of a self-similar structure with triangular capped building blocks [176]. (e) Schematic of the gradient structure of pinecone scales with a gradient of porosity from the inside to the outside surface of the scleroid region [177].

inorganic particles, such as silicon carbide (SiC) [178,179], boron nitride (BN) [180], aluminum nitride (AlN) [181], and various metallic particles, have garnered significant attention for their potential in terms of thermal conductivity and energy dissipation. The mechanical properties, thermal conductivities, and interfacial bonding mechanisms of the constituent particles within the matrix influence their effectiveness in these applications. Madeira et al. [182] reported that the addition of SiC particles improved the damping properties and dynamic modulus of aluminum metal matrix composites and investigated the effect of particle size on these properties. Dong et al. [183] prepared brominated butyl rubber with BN particles and demonstrated that the maximum loss factor can reach 0.95 with 12.3 wt.% BN, while the effective damping temperature range is −41–60 °C. In addition, various types of multiple-particle doping or particle modification have been reported to form special mesoscale feature structures, which are then combined with the matrix to prepare composite materials with extraordinary thermal or electrical performance [184,185]. Figure 23(a), which shows the high thermal conductivity composite material, provides a reference for constructing a variety of

mesoscale feature structures.

One-dimensional fibers (Fig. 23(b)) are another powerful and lightweight solution because of their high modulus, specific strength, and great formability. The presence of natural biological materials has inspired researchers to introduce hierarchical levels, such as textile structures, twisted structures, and nano-stitched laminates, into fiber-reinforced composites (Figs. 23(c)–23(e)). This scheme helps build a wide variety of structural features at the mesolevel, where the interactions of different material components and substructures erupt into multiple damping dissipation mechanisms. The fibers are composed of many microfibrils, which have good viscoelastic behavior and can promote energy dissipation, and more relative displacement between the microfibril sub-layers is generated, leading to more friction and additional dissipation. Meanwhile, the damping of those carbon and plant fibers still involves multiple mechanisms at different levels. Li et al. [186] proposed a multiscale methodology to enhance the damping property via a multilayered composite structure with flax fibers and CNTs. The CNTs penetrate the primary cell wall and interact with the microfibrils in the second layer, improving load transfer from the matrix to the microfibrils. Mofokeng et al. [187] investigated sisal fiber reinforcement composites with poly(lactic acid) (PLA) as the matrix. The dynamic mechanical analysis results clearly show that the introduction of fibers increases the loss factor (Fig. 23(f)). Some fiber-reinforced self-healing composites also have excellent mechanical properties [188,189].

4.4 Composite structures at the macroscale

The rapid development of additive manufacturing in recent years has significantly alleviated technical problems, thereby suggesting that the material–structure–performance integrated design methodology can be used to design and manufacture carefully complex crafted microstructures with "external rigidity but internal chaos" deformation modes. These recently designed microstructures, such as topology optimization-based microstructures (Fig. 24(a)), machine learning-based microstructures (Fig. 24(b)), and biomimetic microstructures (Fig. 24(c)), have provided breakthrough and transformative alternatives to more traditional materials, such as traditional FLD and CLD treatments.

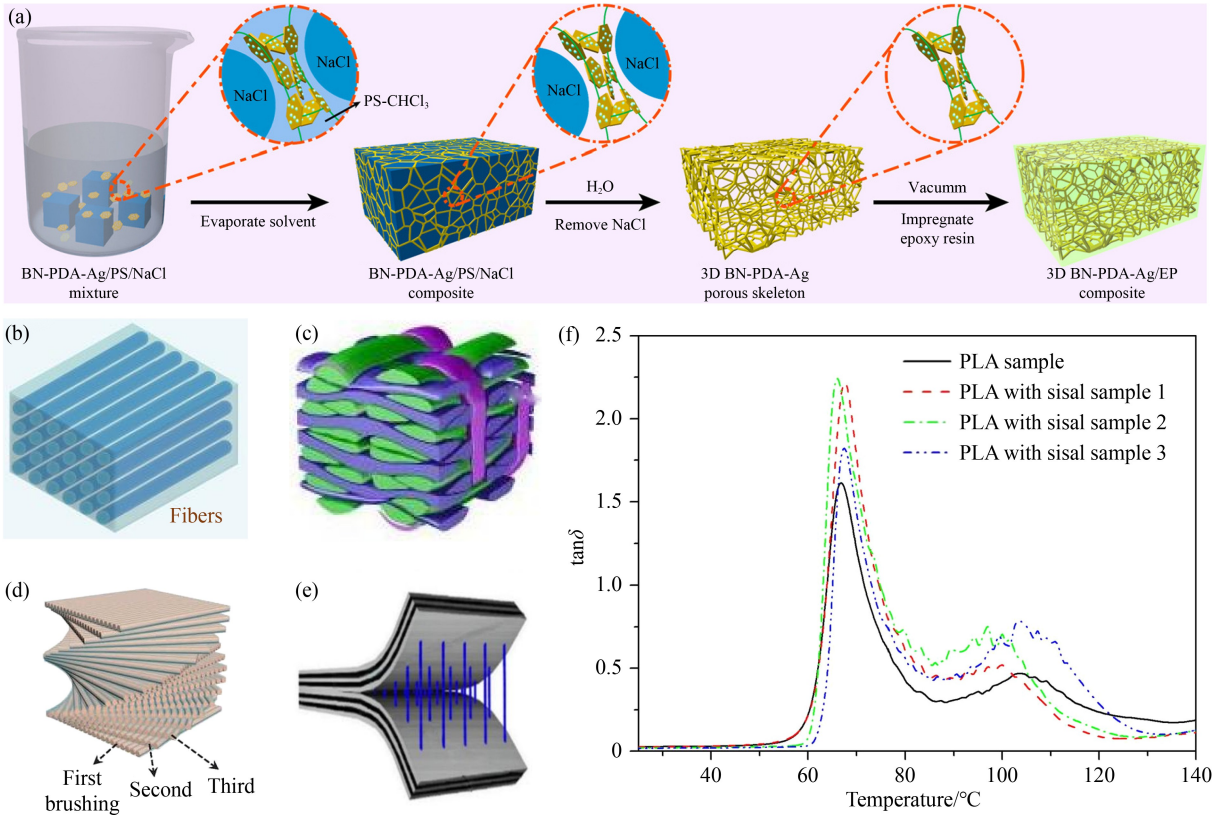

Fig. 23 (a) Schematic of the preparation of BN-PDA-Ag epoxy composites with a three-dimensional interconnected porous network [190]. (b) Schematics of fiber-reinforced composites [191] and some designed feature structures, including (c) textile structures [192], (d) twisted plywood structures [193], and (e) nano-stitched laminates [194]. (f) Temperature-dependent diagram of the loss factor of poly(lactic acid) with sisal fibers [187].

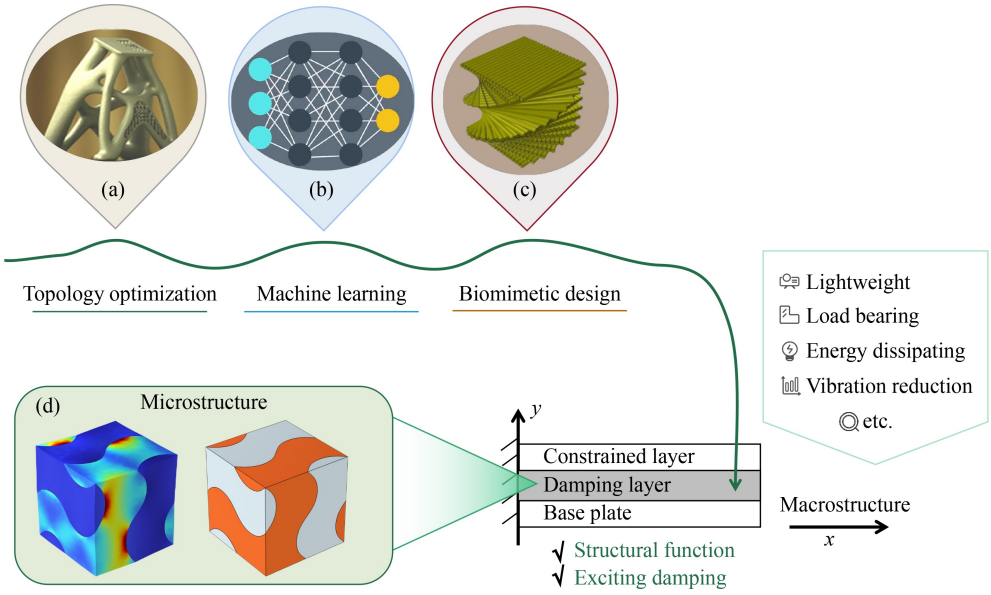

Fig. 24 Design methods to achieve a stiff yet lossy deformation mechanism. (a) A lattice sample after topology optimization [195]. (b) Schematic of a neural network model in machine learning. (c) A bio-inspired helicoidal structure [196]. (d) The damping layer is constructed of a stiff yet lossy structure with the skeleton in gray and the damping filler in orange. In the stress nephogram, the transition from blue to red indicates an increase in stress.

Composites can be engineered at the macroscale to ensure stiffness in the structure phase and allow for energy dissipation in the damping phase. The base structure is responsible for load bearing with high mechanical properties. The deformation generated by the external force is pressed into the damping phases to provide them with the power of relaxation and the excitement of damping mechanisms at each smaller level. Thus, the design idea is to achieve a stiff yet lossy deformation mechanism where the base deforms minimally under external forces, while the internal damping layer deforms considerably to dissipate the energy (Fig. 24(d)). Different methods have been developed to design a damping material (or structure) with high specific damping performance for the composite structure. In this section, a conventional CLD structure with a normal damping material layer is first introduced as a typical composite structure. The novel development of metamaterials is reviewed for their superior advancements as damping fillers.

4.4.1 Traditional application for damping composite structures

As a typical example of a composite structure, a normal CLD structure is a highly effective solution for precision instruments, such as automobiles, aircraft (Fig. 25(a)), and aerospace engines. Its unique ability to reduce vibrations and dampen noise makes it a helpful choice in practice. Theoretical models [197,198] and finite element [199,200] models have been further developed to investigate the dynamic behavior of CLD treatment, and optimization methods have been applied for designing specific structures. The objective design parameters include the type of damping material [201], the shape and size of the layer [202], and the location and number of patches [203]. Topology optimization is popular and effective. Zhang et al. [204] reported that the loss factor of the optimal designed structure is greater than that of the initially designed structure (Fig. 25(b)). However, the damping layer in a traditional CLD structure is oriented only to shear deformation, which greatly limits the excitation of the energy dissipation of the damping phase and its engineering applications.

4.4.2 Trend of extrinsic damping excitation design for damping structures

Recently, emerging metamaterials have realized advantages over conventional materials in terms of their outstanding physical properties. Designing a stiff yet lossy metamaterial for constructing a damping composite structure requires a study of its damping mechanism and how it excites the damping effect of its internal microstructure. The most striking and well-known property is termed metadamping in resonant metamaterials. The dissipation is concentrated in the damping phase of the metamaterial to amplify the dissipation effect, which was studied in depth by Bacquet et al. [206]. For further comprehensive study, the damping performance of a metamaterial includes its unique

wave attenuation in addition to energy dissipation. Mei et al. [207] synthesized the perspectives of the component damping properties (temporal characteristics) and the bandgap (spatial characteristics) of a metamaterial to characterize the wave attenuation properties, which are called spatiotemporal damping. That is, in addition to Bragg scattering, local resonance, and other effects caused by the heterogeneity of the microstructures, the viscoelasticity of the metamaterial components can attenuate elastic or acoustic waves. The spatiotemporal damping mechanism is a coupling effect that covers energy scattering (reflection) and energy dissipation. As shown in Fig. 26, for low dissipation, the spatiotemporal damping mechanism is dominated by energy reflection. In the passband at a low frequency, the increasing dissipation capacity of the material components increases energy dissipation and energy reflection, which enhances the spatiotemporal damping performance in the "valley". Within the bandgap of the local resonance, the inhibition of energy reflection by the dissipation of the components is emphasized, which weakens the spatiotemporal damping performance in the "peak". Within the

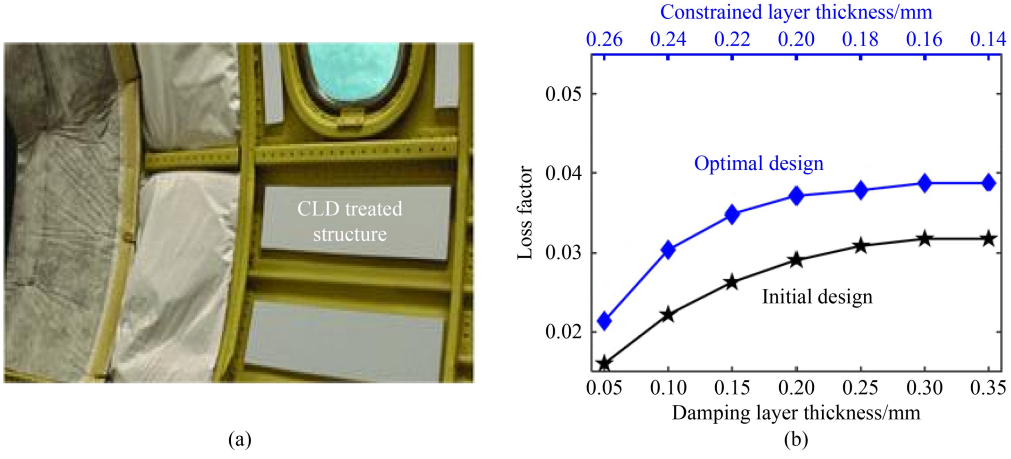

Fig. 25 (a) CLD-treated structure applied in aircraft fuselage [205]. (b) Comparison of the modal loss factor between the topology optimization structure and the initial structure [204].

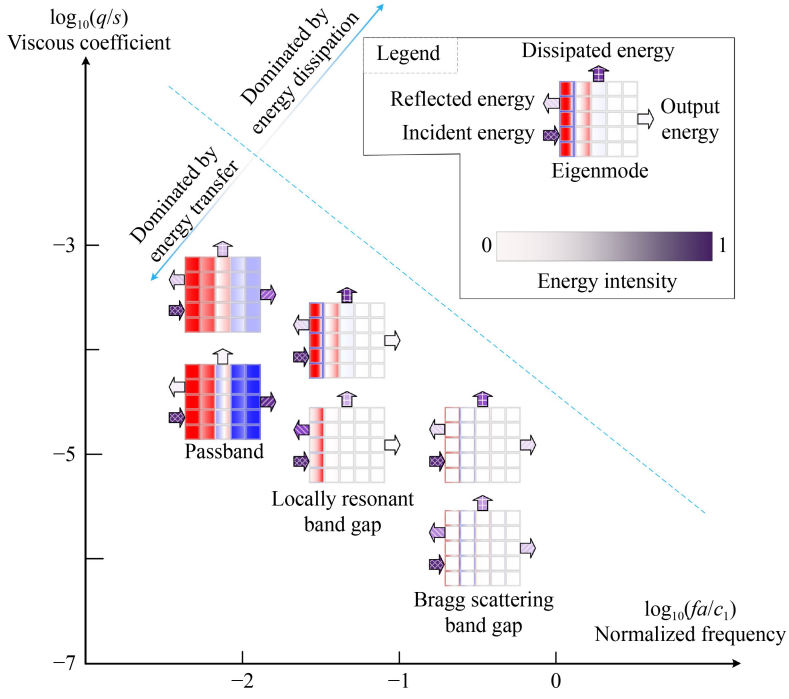

Fig. 26 Diagram of the spatiotemporal damping mechanisms of the viscoelastic metamaterial at different frequencies [207].

Bragg scattering bandgap, the spatiotemporal damping performance is not sensitive to the dissipation effect of the material components. Thus, the coupling effect can be summarized as peak shaving and valley filling. For high dissipation, where energy dissipation is the dominant mechanism, the spatiotemporal damping performance increases with increasing dissipation of the components. The elucidation of this comprehensive mechanism broadens the application prospects for the design of metamaterials for composite structures.

Expanding to a broader set, porous structures composed of periodic or non-periodic lattice arrangements are mostly derived from biomimetic design. The different types of lattice structures are shown in Fig. 27. For example, a honeycomb is typically a two-dimensional lattice structure, whereas three-dimensional lattice structures can be constructed based on triple-periodic minimal surfaces (TPMS), which are widespread in nature [208,209]. A series of sandwich structures with arranged lattice and honeycomb cores were designed in [210–214]. The cellular structure is filled with lightweight damping material, such as polyurethane foam, which has a superior ability to withstand loads and absorb energy. Wei et al. [215] demonstrated that their epoxy/lattice composites have high damping characteristics, with a damping ratio of over 10%. Xu et al. [216] presented carbon fiber-reinforced cellular materials that simultaneously achieve high specific stiffness and damping properties. The lightweight damping phase is intentionally inserted at the center of the selected struts in the lattice (Fig. 28(a)), and experimental methods are conducted to vary the volume fractions of the two constituent materials. The composite structure even has a specific stiffness similar to that of technical ceramics and other composites and can achieve a loss factor of almost two orders of magnitude (Fig. 28(b)).

Recent advances in damping-optimized materials and structures leverage topology optimization and multiscale modeling to achieve superior vibration performance [218–220]. Optimizing layouts at the macro- and microscales (Fig. 29(a)) can lead to a high loss modulus of damping composites within specific frequency ranges. Key innovations include directional damping designs inspired by biomimicry, such as woodpecker beaks, which enhance energy absorption in viscoelastic composites [221], and multi-phase materials with optimal soft-to-stiff damping ratios that balance stiffness and damping. Concurrent optimization frameworks for free-layer and shell structures integrate macro- and microscale layouts to reduce vibrations under harmonic excitations [222], employing efficient computational techniques, such as reduced-order modeling and sensitivity-driven analysis. These studies collectively demonstrate the potential of advanced damping designs via multiscale topology optimization for applications in automotive, aerospace, and vibration control systems, offering

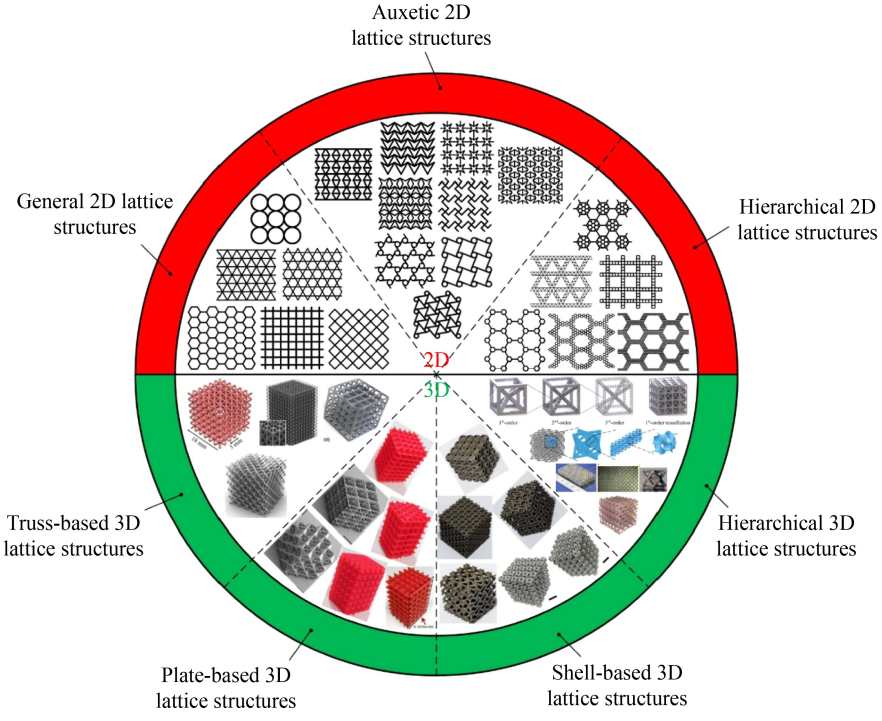

Fig. 27 Different types of lattice structures [217].

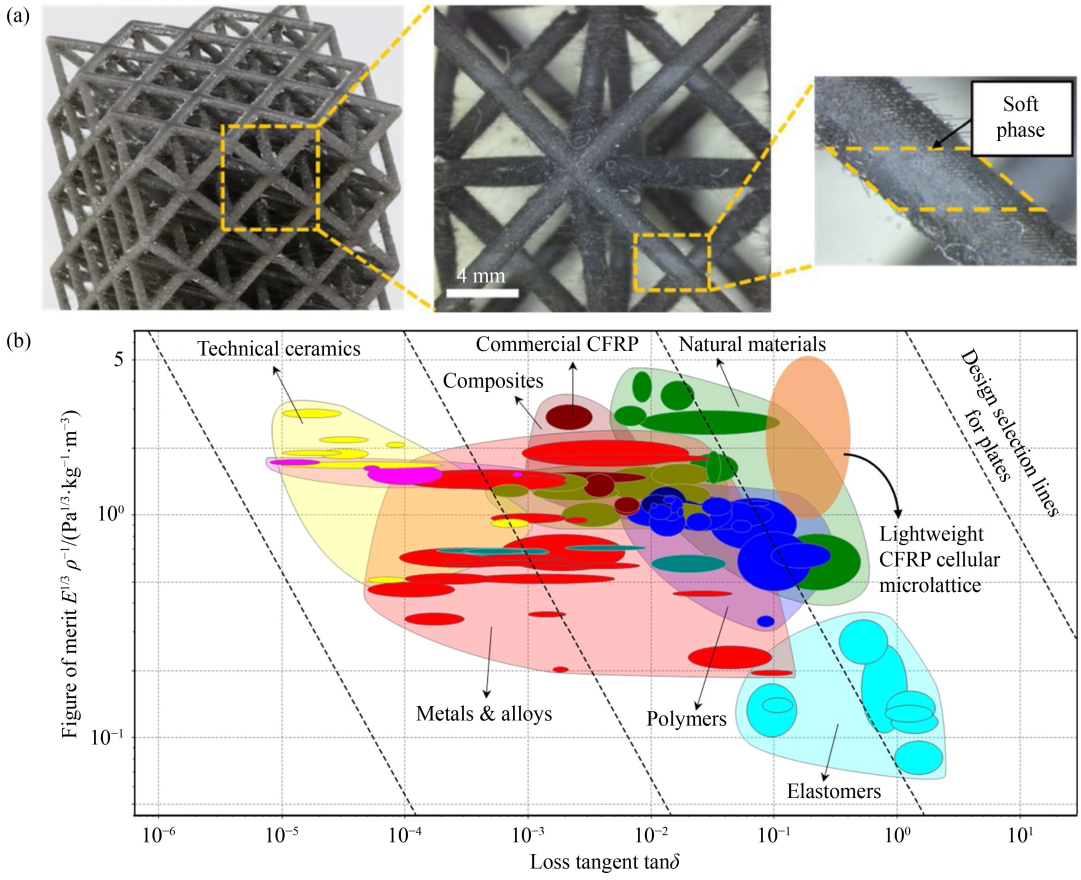

Fig. 28 (a) Lightweight soft phase in a microlattice of the honeycomb structure and (b) comparison of the loss factor and specific stiffness between CFRP cellular materials and common materials, where E is the effective modulus, and ρ denotes the density [216]. CFRP: carbon fiber reinforced polymer.

improved performance and practical scalability.

The development of machine learning offers great help in theoretical modeling for calibrating parameters and describing mechanical behavior, contributing to the lattice design of porous materials [223–225]. Challapalli et al. [226] discovered optimal lattices via machine learning and novel inverse design techniques. Three-dimensional printing helps manufacture different types of lattices (Fig. 29(b)). The designed structures surpass the damping performance and are lightweight biomimetic structures, such as honeycombs. Abu-Mualla et al. [227] proposed a data-driven framework for the inverse design of manufacturable cellular mechanical metamaterials. Using a physics-guided neural network and a dataset based on cubic symmetries, the method can predict anisotropic stiffness components with high accuracy and computational efficiency, outperforming traditional approaches. Other inverse design networks have also been developed for scalable and precise control over mechanical behavior, offering promising applications in wearable devices, soft robotics, and advanced sensors [228,229].

5 Stiffness mechanisms of self-healing polymers

Although the stiffness and strength of damping composite structures are ensured mainly by the base structure, the energy storage capacity of the damping material is also crucial. As mentioned earlier, damping materials need to store energy, i.e., have enough dynamic stiffness, to dissipate mechanical energy efficiently. Therefore, focusing on polymer materials is necessary for investigating the stiffness enhancement mechanism of damping materials. These opportunities allow new design strategies to be explored, thereby achieving high specific damping performance for balancing stiffness and damping.

The entropic force of crosslinking in polymers is a factor in their resistance to deformation of their network structure. As shown in Fig. 30(a), each crosslinking point is essentially a physical or chemical bond, and the crosslinking strength determines the structural stiffness. The chains are more difficult to deform and break because they are connected by strong and irreversible chemical bonds. Figure 30(b) shows that nanofillers can absorb polymer chains and

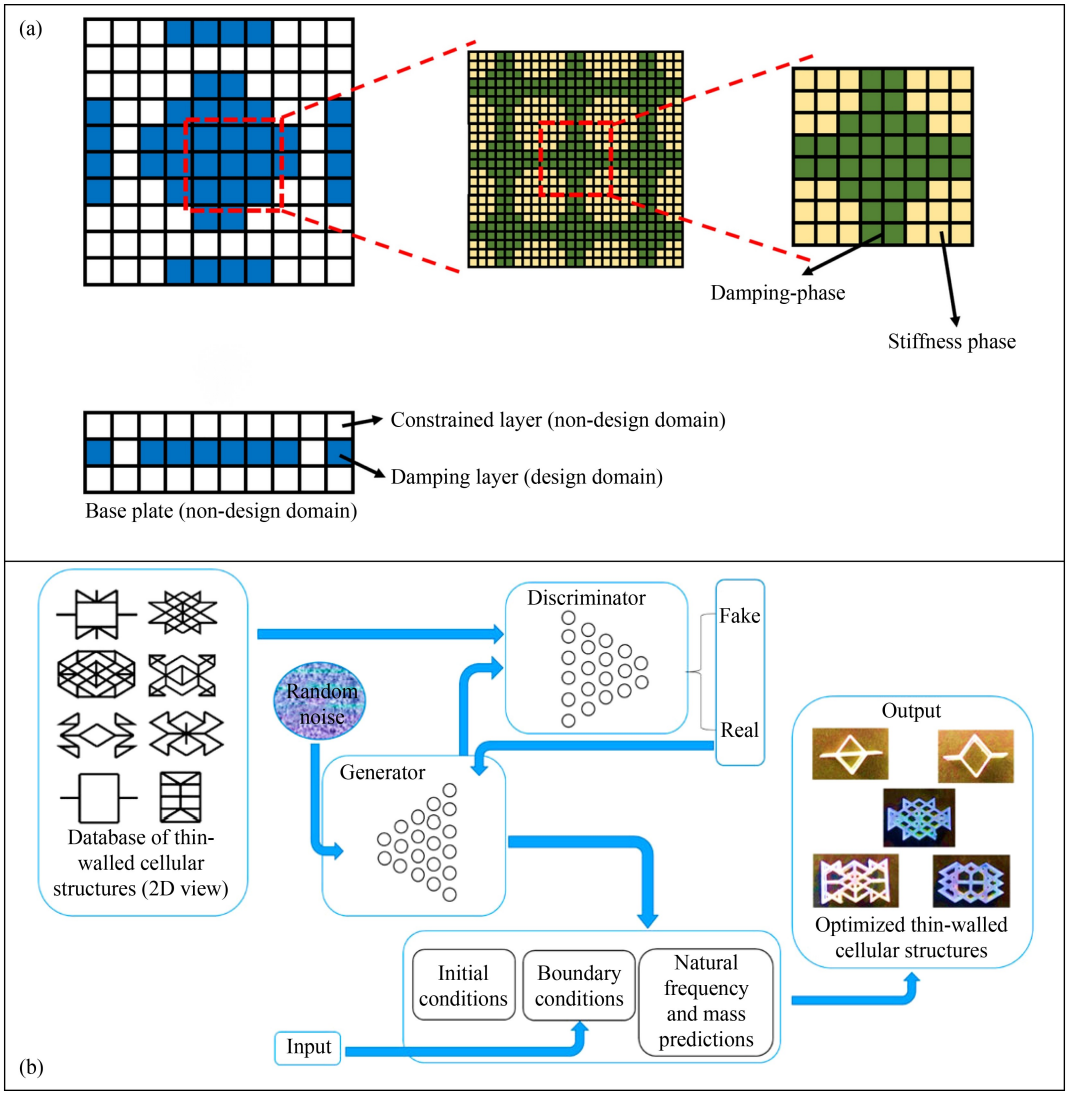

Fig. 29 (a) Schematic of a damping structure with a microstructured composite composed of a stiffness phase and a damping phase [220]. (b) Schematic of the design procedure of thin-walled lattices in the metamaterial structure [226].

form interfaces. This situation further increases the forces and entropy within the structure. Thus, the external force required for structural deformation is greater, improving the stiffness performance. In addition, the interlocking structure (Fig. 30(c)) consists of two or more bonded molecular fragments. They are locked together by mechanical bonds to form topological constraints that prevent separation. An increase in entropy can also be achieved by superimposing and mixing multiple polymer networks to increase the crosslinking density (Fig. 30(d)) via a double network, curing, or polymerization. Complex chain crosslinking can effectively resist the risk of deformation and damage.

5.1 Entropic forces in crosslinking

At the molecular level, the structure of polymeric materials is a three-dimensional network formed by connecting polymer chains with covalent or non-covalent bonds. The energy required for deformation and fracture increases with increasing bonding energy. Meanwhile, high-stiffness polymers similar to the matrix generate more entropy force in the structure. Combining multiple covalent and non-covalent bonds is also feasible to compensate for the weak energy of a single connection so that the dynamic structure can remain strong and stable [230–234].

The introduction of molecular chains with strong internal forces can also increase the entropy force within the structure. Li et al. [52] designed a disulfide-bonded eugenol-based dynamic covalent epoxy resin network with a tightly crosslinked structure. The prepared epoxy resin has a Young's modulus of approximately 2.2 GPa and a high loss factor close to 0.9, reflecting the excellent stiffness properties of the

material and demonstrating a self-healing rate of up to 84.8%. Kim et al. [235] reported that the use of 4-aminophenyl disulfide (4-AFD) with a tightly packed structure (Fig. 31(a)) as a hardener can increase intermolecular forces and hinder the movement of molecular chains and the self-healing behavior of the material. Alternatively, 2-aminophenyl disulfide (2-AFD) with a linear structure (Fig. 31(b)) can produce a more relaxed conformation but leads to lower stiffness. Martinez-Diaz et al. [236] compared the modulus of vitrimers containing 2-AFD and 4-AFD (Fig. 31(c)). Wang et al. [65] intensively investigated Schiff base covalent adaptive networks and designed combinations of epoxy resins and polyimides. The highly π-conjugated Schiff base structure and hydrogen bonding result in high stiffness (2.112 GPa), which is greater than that of conventional epoxy resin-based polymers (2.02 GPa). However, the motility of the structure is also limited, leading to low damping. Its loss factor (0.3) is lower than that of conventional epoxy resin (0.8). In addition, the mechanical properties of the prepared material did not decrease significantly after healing, but its modulus even slightly increased.

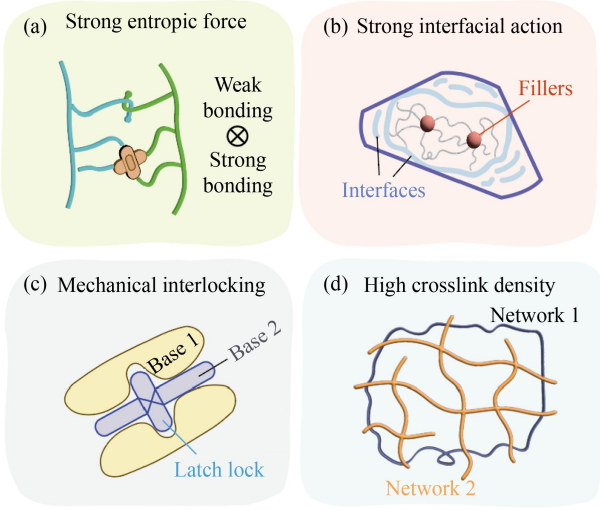

Fig. 30 Mechanisms for improving the stiffness of polymers, including (a) strong entropic forces between crosslinkers, (b) the introduction of strong interfaces to increase the force, (c) the design of mechanical interlocking structures, and (d) an increase in the crosslinking density.

5.2 Interaction of strong interfaces

In addition to the viscous motion and inelastic deformation that dissipates energy, the adsorption and interlocking of interfaces can effectively resist tensile deformation and provide rigidity to the structure. However, in contrast to the mechanism by which the interface affects the stiffness of traditional composite materials [237–241], its effect on self-healing materials still needs to be reported. Li et al.

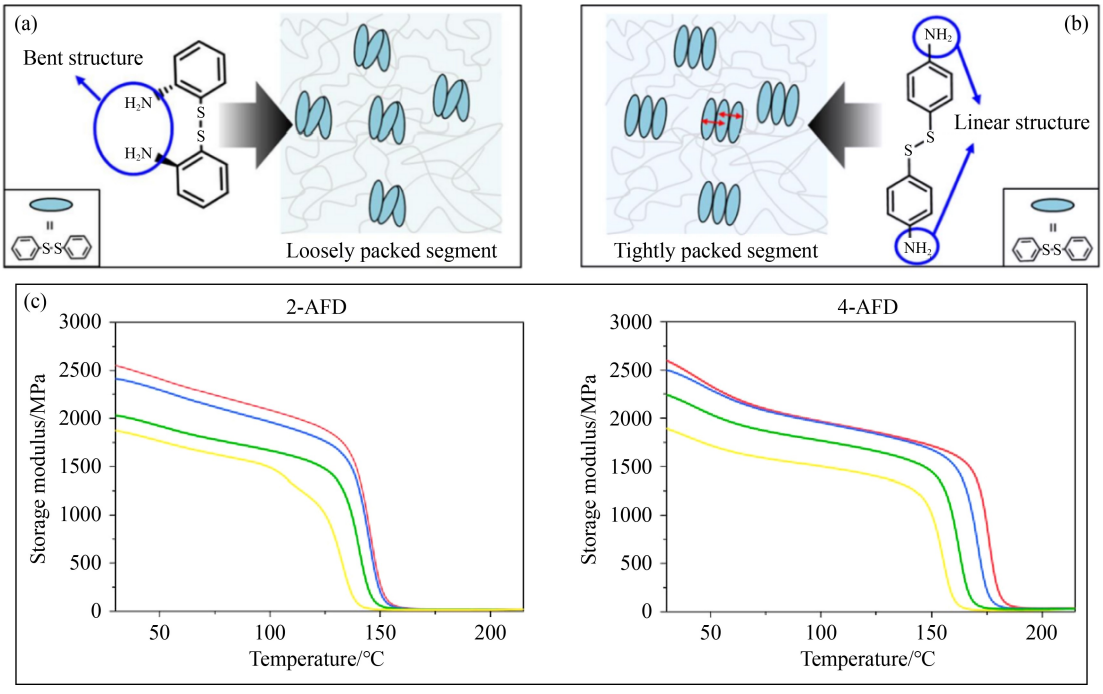

Fig. 31 Schematics of (a) loosely structured 2-AFD and (b) tightly structured 4-AFD [235]. (c) Storage modulus comparison diagrams of vitrimers containing 2-AFD and 4-AFD, where different colored curves represent different samples [236].

[242] considered the effects of the interface, reinforcement phase, and stacking order on the structural deformation of carbon fiber reinforced polymers. They proposed an analytical method to predict the stiffness behavior of composites by introducing an interfacial strengthening factor, showing that the aggregated carbon fiber layers possess stronger adhesive interfaces and significantly improve the tensile strength and stiffness of the material. Lee et al. [243] predicted the elastic modulus of PA6/SiC nanocomposites via multiscale modeling and investigated the applicability of two interface models and their effects on structural stiffness. The elastic modulus increases with decreasing nanoparticle size when the interface is dense and stiff. Demir et al. [244] noted that the interfacial adhesion between carbon fibers and the polymer matrix can significantly limit the mechanical properties of the composite and thus proposed a surface engineering method to chemically modify the carbon fibers to enhance the interfacial interaction and improve the strength and stiffness of the structure. Guru et al. [245] used molecular dynamics to determine the elastic characteristics of the matrix, interfacial energy, and interfacial gap. They created a three-dimensional volume cell consisting of an epoxy matrix, single-walled CNTs, and their interfaces. Moreover, the influences of the interfacial thickness and stiffness on the Young's modulus of the nanocomposites were investigated. The effect of the interfacial stiffness on the elastic properties of the nanocomposites was more pronounced than that of the interfacial thickness.

5.3 Mechanical interlocking structure

Interlocking structures, such as lasso peptides, are prevalent in organisms, and engineering applications involve tools such as chains and lockets. Interlocking structures are formed by entangling two or more components in space via mechanical bonds to enhance structural stability, integrity, and rigidity. Duan et al. [246] developed novel three-dimensional pillared graphene nanostructures (PGNs) as reinforcements in a polyethylene (PE) matrix. PGNs were constructed by inserting CNTs vertically between graphene sheets via covalent bonding, which was cross-linked with the matrix to produce an interlocking effect. In particular, the elastic modulus of the composites is not only positively correlated with the mass fraction of PGNs but also highly correlated with the degree of interlocking phenomenon occurring in the structure. In addition, mechanically interlocked molecules (MIMs) covalently polymerize with the matrix, which is one of the emerging research directions for polymer networks [247–251]. Chen et al. [252] reviewed the synthesis, properties, and applications of mechanically interlocked polymers based on rotaxane structures and summarized the excellent properties of the introduction of rotaxanes to the polymers. In terms of absorption, the sliding of rotaxane molecules between rings and axes introduces a unique energy dissipation mechanism, which enhances the damping properties of the structure. As the mechanical bonds cannot be reformed, the recycling and reprocessing of polymers with conventional mechanical interlocking structures still need improvement. However, Zhao et al. [253] coupled mechanical bonding with dynamic covalent bonding and proposed a new concept of a mechanically interlocked vitrimer (Fig. 32(a)). The prepared vitrimer MIV-1 achieved a Young's modulus of 18.5 MPa in stiffness, which is much higher than that of conventional vitrimers (Fig. 32(b)), and had a damping capacity (ratio of energy output to input) of 98%. The recycled material could retain good chemical integrity and mechanical properties.

5.4 Crosslinking density of the network

Another mechanism to improve the stiffness of polymers is to increase the crosslinking density of their molecular chains. Different molecular clusters can be crosslinked by copolymerization, curing, and mixing. This forms a high-density multi-chain structure in which long chains interlace and interpenetrate with short chains (Fig. 30(d)). The complex network structure hinders the internal rotation of chains. This situation reduces the structural flexibility, and it is challenging to converge to the ordered state in Fig. 8. Moreover, the longer the molecular chain is, the greater the number of conformations, and although the short chains are susceptible to external forces in space and change their morphology, the presence of long chains can still resist deformation. The crosslinking density is highly correlated with the glass transition temperature and modulus [254–257].

Isogai and Hayashi [258], in a recent study, suggested that the number of branching chains at the same point is significant for the performance of self-healing polymers and that polymers with more branches have a higher crosslinking density and higher modulus (Fig. 33). Hajj et al. [259] also revealed a significant effect of density on relaxation time by analyzing the viscoelasticity of network structures containing imine bonds with different densities. Han et al. [44] synthesized different groups of hyperbranched epoxy (HBE): HBE-1 and HBE-2. HBE-2 has a higher molecular weight and more reactive groups than HBE-1, leading to a higher crosslinking density. A vitrimer based on DER epoxy resin, which has the highest crosslinking density and

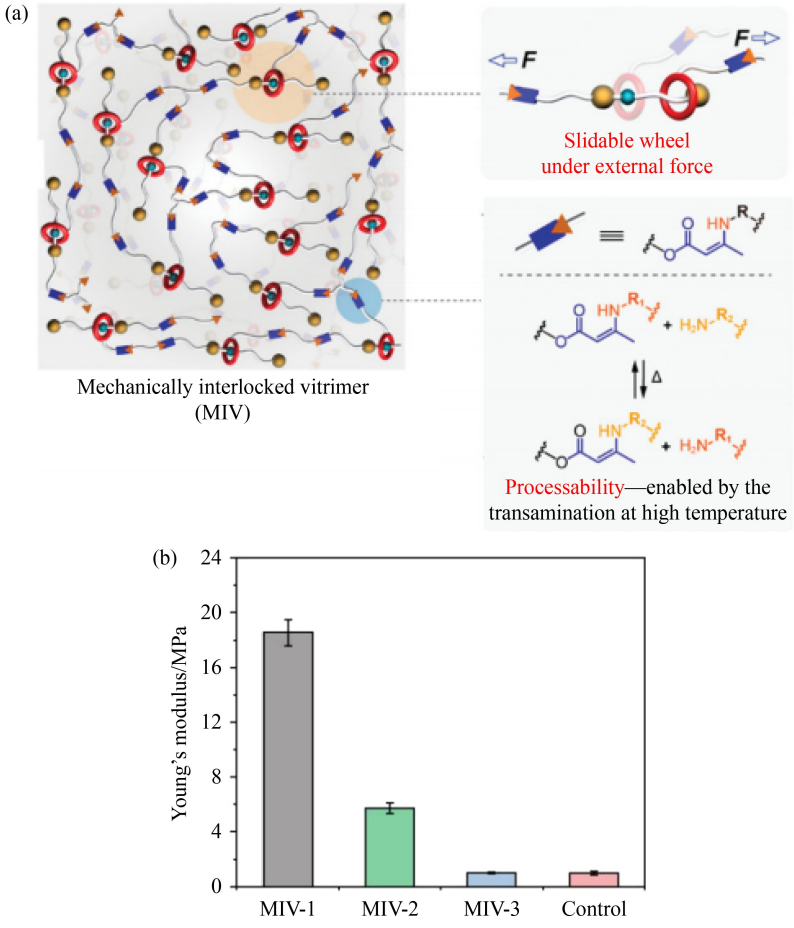

Fig. 32 (a) Schematic of the slidable MIV structure and (b) its Young's modulus [253].

modulus, was also prepared (Fig. 34). Liu et al. [66] synthesized a new high-performance tri-epoxy (TEP) resin in 2018 and cured TEP with anhydride monomers catalyzed by zinc ions (Fig. 35). The elastic modulus of the cured epoxy increases from 1.63 to 2.11 GPa, but the loss factor is only 0.4, which is lower than that of conventional bisphenol-A epoxy resins. The cracks in the material could be effectively repaired within 10 min, with a healing efficiency of 90%. An et al. [85] constructed vitrimer systems with diselenide bonds and synthesized three epoxy resin networks of increasing density, Se-EP-D, C-EP-D, and Se-EP-F, and the densest Se-EP-F system had the highest elastic modulus of 3.26 GPa.

In studies of hydrogels [260–264], a double network structure (Fig. 36) with high brittleness and poor performance has been proposed to effectively improve the shortcomings of conventional structures. The double network is composed of two interconnected networks with noticeably different yet intertwined properties, one of which is tightly crosslinked and can absorb energy, providing high strength to the structure. Conversely, the other segment of the network is loosely crosslinked and is not easily broken under stress, which then increases the toughness of the structure. In the current research, the double network has received extensive attention and development and is an essential means of application and realization in the stiffness mechanism.

6 Design principles for specific damping performance

Inspired by the multiscale mechanisms of bio-composites and artificial composites, the following three principles can be used to guide the design of the specific damping performance of artificial composites.

a) The damping properties of composites can be improved by utilizing multiple damping sources of soft materials at the nanoscale (physical damping, chemical damping, and plastic damping mechanisms), while the synergistic effects of hard and soft phases can significantly enhance the specific damping properties of composites, including high energy storage and mechanical energy dissipation.

b) At each level of the structural hierarchy in composites, the microstructure of the hard phase

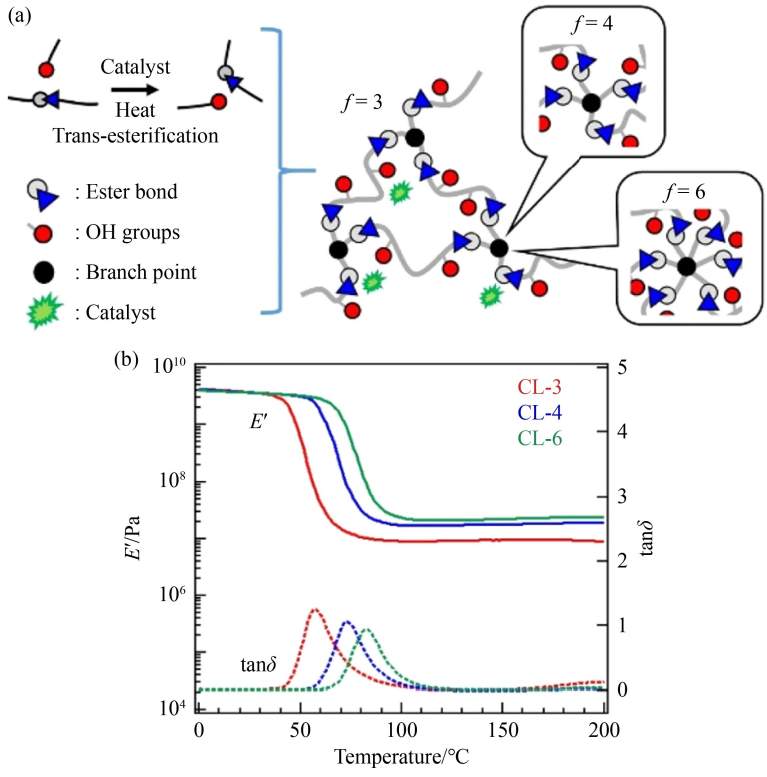

Fig. 33 (a) Schematics of crosslinkers containing three branches CL-3, four branches CL-4, and six branches CL-6 and (b) comparison of their storage moduli and loss factors [258].

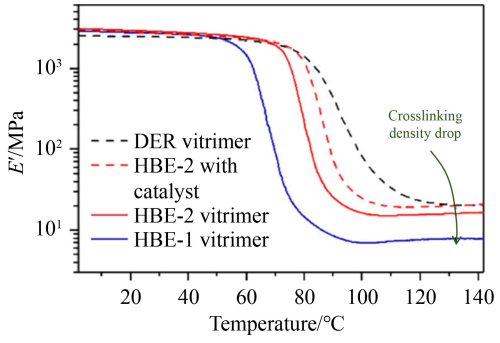

Fig. 34 Storage moduli of vitrimers with different crosslinking densities as a function of temperature [44].

needs to be rationally designed to exploit the dual roles of the constituents of the hard phase itself and the damping excitation effect by guiding the hard phase to drive the deformation mechanism.

c) Although microscale and mesoscale hard fillers have the same damping excitation mechanisms (adhesion, slip, and press-in effects), they have distinct roles in enhancing the specific damping performance of artificial composites. Owing to their discrete–continuous coupled structural features, microscale hard fillers are the least invasive and are expected to improve damping performance without sacrificing mechanical properties or structural integrity. However, mesoscale hard fillers can present

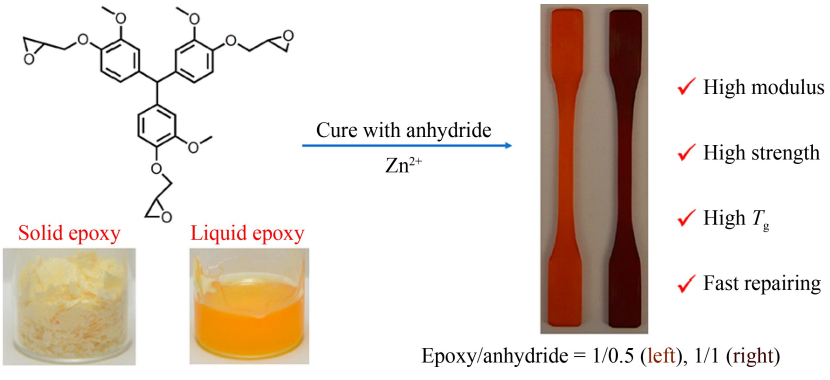

Fig. 35 Synthesis and properties of a self-healing tri-epoxy resin [66].

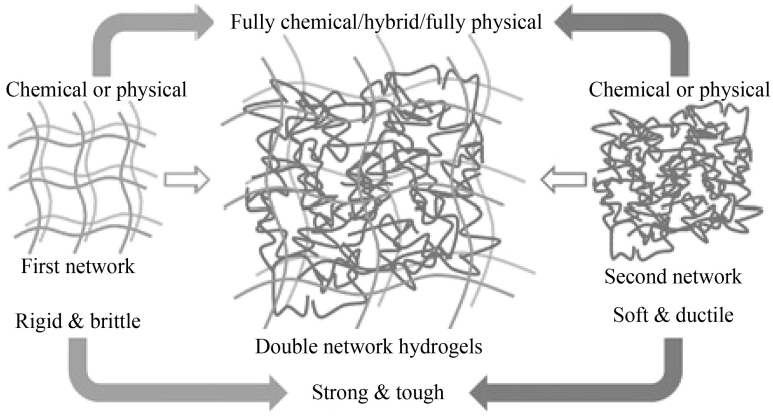

Fig. 36 Double network properties of hydrogels [265].

larger microstructural features and thus can improve damping performance at lower frequencies than microscale hard fillers can.

7 Summary and outlook

Self-healing materials, which are widely developed in modern engineering applications, can automatically detect failure and self-repair to prevent potential damage caused by cracking and effectively extend the service life. Moreover, the self-healing property itself is a chemical reaction that requires energy dissipation, so it can be exploited to improve damping capabilities.

The continuous pursuit of extremely lightweight and multi-functional integrated designs in modern industries requires that structural materials are not limited to ensuring the structural load-bearing function of lightweight designs; rather, they must have high mechanical properties and high damping capabilities. For the damping phase of structure–damping composites, their specific damping performance (high stiffness and high damping) is a key factor; however, their stiff yet lossy performance conflicts with self-healing properties.

In this review, the mechanisms of stiffness, damping, and self-healing are summarized. The synthesis methods and performance of some reported self-healing materials are reviewed. Under the premise of ensuring high self-healing efficiency, the stiffness–loss map of materials based on different self-healing mechanisms is evaluated (Fig. 37). Self-healing materials have slight advantages over traditional engineering materials, with a figure of merit above the guideline of 0.6 GPa. That is, damping composite materials or structures involving self-healing constituents can achieve a surpassingly stiff yet lossy performance and therefore can be integrated into a structure-damping composite

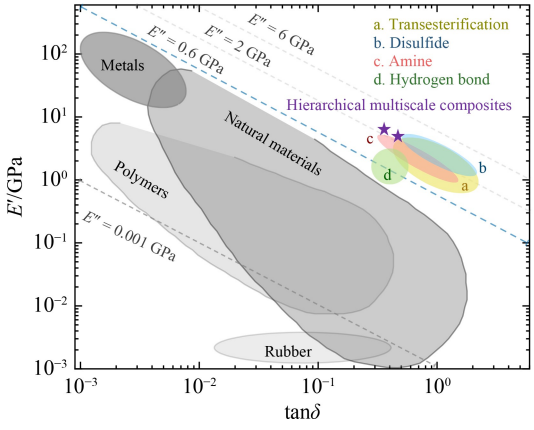

Fig. 37 Distribution of the storage modulus E' and loss factor $\tan\delta$ of self-healing composites based on different self-healing mechanisms.

structure with high mechanical properties and superior specific damping performance. Therefore, damping composite structures involving self-healing constituents are expected to be widely applied in structural engineering in modern industries, such as the aviation, aerospace, navigation, automobile, and robot fields.

For the research and development of self-healing materials and structure-damping composite structures in engineering, this work presents the following outlook. Inspired by the multilevel structure of bones at multiple spatial and temporal scales, their unique architecture (Fig. 38) sets them apart from traditional engineering and biological materials as marks of hierarchical structure designed by Feng et al. [267] (Fig. 37), showing an impressive figure of merit. The use of a multiscale design method can lead to the biomimetic construction of materials and composite structures with good mechanical properties and self-healing capabilities. The bottom-up design suggestions are divided into several points:

a) At the nanolevel, dynamic bonds are introduced

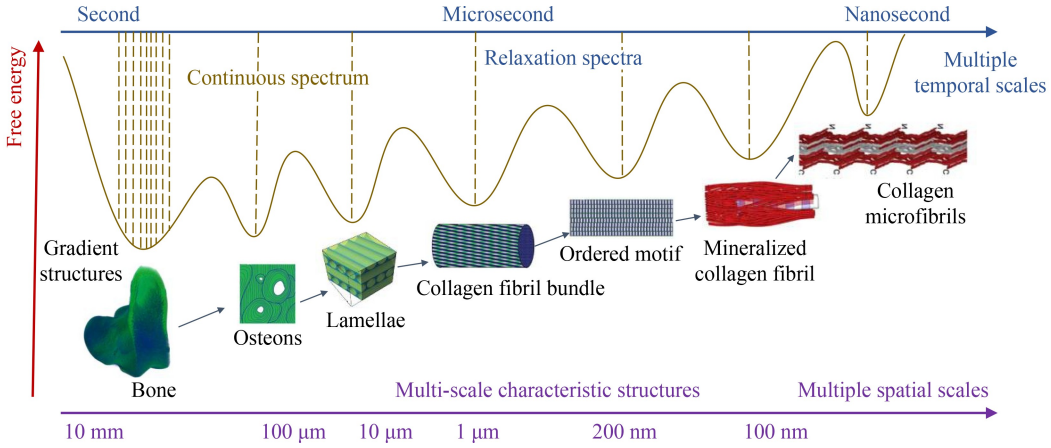

Fig. 38 Multilevel structure of bones at multiple temporal–spatial scales, forming a wide and continuous relaxation spectrum. Illustrations are adapted from Reznikov et al. [266].

as soft matter to provide additional intrinsic chemical damping sources and achieve self-healing, while the original polymer network still provides a stable material structure to provide stiffness and strength. Those dangling chains and multiple motion units benefit chain scission and reformation, which are simulated by mechanical energy, to relaxation. However, the complementary correlation between the mechanical and self-healing properties needs further explanation. We suggest elucidating the characteristics of relaxation behavior during self-healing and ultimately exploring the influence of design parameters on stiffness, damping, and self-healing performance via systematic experimental methods.

b) At the microlevel, various stiff fillers are introduced as hard matter. A modulus-mismatching interface can be formed to provide extrinsic deformation-driven modes for relaxation and sufficient interface damping. The relaxation spectra of the characteristic structure at each level can be identified via experimental and simulation analyses. Dissecting their associations and coupling mechanisms can help develop methods for designing composites with wide frequency spectra (corresponding to a wide temperature range) in engineering applications.

c) At the meso- and macrolevels, metamaterials with microstructures can be processed by additive manufacturing as the damping layer for composite structures. However, the integration of damping composite materials or structures with self-healing capacity into a structure–damping composite structure has yet to be reported. In the complex conditions of modern engineering, the structure–damping composite needs to maximally excite the damping capacity of viscoelastic fillers. Multiple temporal–spatial numerical models of energy dissipation for self-healing elements, characteristic features, and multilevel structures constitute one of the main research directions. Then, a quantitative prediction method for damping performance can be further developed to realize the design innovation of characteristic structures at each level, achieving highly stiff yet lossy performance so that they can be widely applied in structural engineering in modern industries.

The effective damping performance of a damping composite structure relies not only on its intrinsic damping sources at the nanoscale but also on its extrinsic deformation-driving modes at the macroscale. The intrinsic damping sources and extrinsic deformation driving modes can be integrated into a material–structure–performance integrated design methodology, which is expected to provide breakthrough and transformative alternatives to more traditional materials, such as traditional FLD and CLD treatments.

The ability of the material–structure–performance integrated design strategy to overcome the critical bottleneck of attaining high stiffness and high damping (high specific damping) would unlock the many opportunities offered by the broad class of damping composite materials, thereby enabling a fundamental advancement in a variety of pivotal vibration-induced damping applications, including instrument operation accuracy, vibration and noise control, equipment reliability, and the service life of components (or machines).

Furthermore, highly specific damping materials can be integrated into a base material/structure with high mechanical performance (i.e., high strength and high toughness), which is expected to achieve high mechanical properties and high specific damping, thereby enabling a fundamental leap forward in a variety of pivotal applications, including but not limited to lightweight components for aviation,

aerospace, navigation, automobile, and robot applications.

Nomenclature

Abbreviations

AFD	Aminophenyl disulfide
AlN	Aluminum nitride
BN	Boron nitride
CAN	Covalent adaptive network
CLD	Constrained layer damping
CNT	Carbon nanotube
CTH	Close-then-heal
FLD	Free layer damping
HBE	Hyperbranched epoxy
MIM	Mechanically interlocked molecule
PE	Polyethylene
PGN	Pillared graphene nanostructures
PLA	Poly(lactic acid)
SiC	Silicon carbide

Acknowledgements This work was supported by the National Natural Science Foundation of China (Grant No. 52175095) and the Young Top-notch Talent Cultivation Program of Hubei Province of China.

Conflict of Interest The authors declare no conflict of interest.

References

1. Rao M D. Recent applications of viscoelastic damping for noise control in automobiles and commercial airplanes. Journal of Sound and Vibration, 2003, 262(3): 457–474
2. Cremer L, Heckl M. Structure-borne Sound: Structural Vibrations and Sound Radiation at Audio Frequencies. Springer Science & Business Media, 2013, 1–3
3. Lakes R S. High damping composite materials: effect of structural hierarchy. Journal of Composite Materials, 2002, 36(3): 287–297
4. Woigk W, Poloni E, Grossman M, Bouville F, Masania K, Studart A R. Nacre-like composites with superior specific damping performance. Proceedings of the National Academy of Sciences of the United States of America, 2022, 119(31): e2118868119
5. Xu C, Li L. A surpassingly stiff yet lossy multiscale nanocomposite inspired by bio-architecture. Materials Today. Communications, 2023, 35: 105982
6. Wang F, Li L, Jiang X, Tang H, Wang X, Hu Y. High damping and modulus of aluminum matrix composites reinforced with carbon nanotube skeleton inspired by diamond lattice. Composite Structures, 2023, 323: 117451
7. Gu D, Shi X, Poprawe R, Bourell D L, Setchi R, Zhu J. Material-structure-performance integrated laser-metal additive manufacturing. Science, 2021, 372(6545): eabg1487
8. Garg A, Sharma A, Zheng W, Li L. A review on artificial intelligence-enabled mechanical analysis of 3D printed and FEM-modelled auxetic metamaterials. Virtual and Physical Prototyping, 2025, 20(1): e2445712
9. Chatzimichali A P, Potter K D. From composite material technologies to composite products: a cross-sectorial reflection on technology transitions and production capability. Translational materials research, 2015, 2(2): 026001
10. Aïssa B, Therriault D, Haddad E, Jamroz W. Self-healing materials systems: overview of major approaches and recent developed technologies. Advances in Materials Science and Engineering, 2012, 2012: 1–17
11. Xu C, Feng H, Li Y, Li L. Design of surpassing damping and modulus nanocomposites with tunable frequency range via hierarchical bio-architecture. Polymer Composites, 2024, 45(5): 4374–4388
12. Yu K, Shi Q, Dunn M L, Wang T, Qi H J. Carbon fiber reinforced thermoset composite with near 100% recyclability. Advanced Functional Materials, 2016, 26(33): 6098–6106
13. Capelot M, Montarnal D, Tournilhac F, Leibler L. Metal-catalyzed transesterification for healing and assembling of thermosets. Journal of the American Chemical Society, 2012, 134(18): 7664–7667
14. Wang W, Yeung Kelvin W K. Bone grafts and biomaterials substitutes for bone defect repair: a review. Bioactive Materials, 2017, 2(4): 224–247
15. Kheyrandish M R, Mir S M, Sheikh Arabi M. DNA repair pathways as a novel therapeutic strategy in esophageal cancer: a review study. Cancer reports, 2022, 5(11): e1716
16. Patrick J F, Robb M J, Sottos N R, Moore J S, White S R. Polymers with autonomous life-cycle control.

Nature, 2016, 540(7633): 363–370
17. Willocq B, Odent J, Dubois P, Raquez J M. Advances in intrinsic self-healing polyurethanes and related composites. RSC Advances, 2020, 10(23): 13766–13782
18. Mihashi H, Nishiwaki T. Development of engineered self-healing and self-repairing concrete-state-of-the-art report. Journal of Advanced Concrete Technology, 2012, 10(5): 170–184
19. Alazhari M S. The effect of microbiological agents on the efficiency of bio-based repair systems for concrete. Dissertation for the Doctoral Degree. Bath: University of Bath, 2017, 28–29
20. Huang Y, Wang X, Sheng M, Qin D, Ren J, Zhou X, Zhu J, Xing F. Dynamic behavior of microcapsule-based self-healing concrete subjected to impact loading. Construction & Building Materials, 2021, 301: 124322
21. Barbu A M, Stoian M M. Innovative technologies in constructions. Self-repairing concrete used in road infrastructure. IOP Conference Series. Earth and Environmental Science, 2021, 664(1): 012082
22. Reddy P, Kavyateja B. Experimental study on strength parameters of self repairing concrete. Annales de Chimie - Science des Materiaux, 2019, 43(5): 305–310
23. Zhang X, Qian C. Engineering application of microbial self-healing concrete in lock channel wall. Marine Georesources and Geotechnology, 2022, 40(1): 96–103
24. Rule J D, Sottos N R, White S R. Effect of microcapsule size on the performance of self-healing polymers. Polymer, 2007, 48(12): 3520–3529
25. Zako M, Takano N. Intelligent material systems using epoxy particles to repair microcracks and delamination damage in GFRP. Journal of Intelligent Material Systems and Structures, 1999, 10(10): 836–841
26. Hayes S A, Jones F R, Marshiya K, Zhang W. A self-healing thermosetting composite material. Composites Part A: Applied Science and Manufacturing, 2007, 38(4): 1116–1120
27. Lee M W, An S, Yoon S S, Yarin A L. Advances in self-healing materials based on vascular networks with mechanical self-repair characteristics. Advances in Colloid and Interface Science, 2018, 252: 21–37
28. Toohey K S, White S R, Sottos N R. Microvascular networks for self-healing polymer coatings. In: Fifteenth United States National Congress of Theoretical and Applied Mechanics, 2006
29. Williams H R, Trask R S, Bond I P. Design of vascular networks for self-healing sandwich structures. In: Proceedings of the 1st International Conference on Self-healing Materials. Noordwijk aan Zee: Springer, 2007, 18–20
30. Koh E, Kim N K, Shin J, Kim Y W. Polyurethane microcapsules for self-healing paint coatings. RSC Advances, 2014, 4(31): 16214–16223
31. Scheutz G M, Lessard J J, Sims M B, Sumerlin B S. Adaptable crosslinks in polymeric materials: resolving the intersection of thermoplastics and thermosets. Journal of the American Chemical Society, 2019, 141(41): 16181–16196
32. Li L, Chen X, Torkelson J M. Covalent adaptive networks for enhanced adhesion: Exploiting disulfide dynamic chemistry and annealing during application. ACS Applied Polymer Materials, 2020, 2(11): 4658–4665
33. Zou W, Dong J, Luo Y, Zhao Q, Xie T. Dynamic covalent polymer networks: from old chemistry to modern day innovations. Advanced Materials, 2017, 29(14): 1606100
34. Bergman S D, Wudl F. Mendable polymers. Journal of Materials Chemistry, 2008, 18(1): 41–62
35. Montarnal D, Capelot M, Tournilhac F, Leibler L. Silica-like malleable materials from permanent organic networks. Science, 2011, 334(6058): 965–968
36. Ahmadi M, Hanifpour A, Ghiassinejad S, van Ruymbeke E. Polyolefins vitrimers: design principles and applications. Chemistry of Materials, 2022, 34(23): 10249–10271
37. Alabiso W, Schlögl S. The impact of vitrimers on the industry of the future: chemistry, properties and sustainable forward-looking applications. Polymers, 2020, 12(8): 1660
38. Zheng J, Png Z M, Ng S H, Tham G X, Ye E, Goh S S, Loh X J, Li Z. Vitrimers: current research trends and their emerging applications. Materials Today, 2021, 51: 586–625
39. Yang Y, Pei Z, Zhang X, Tao L, Wei Y, Ji Y. Carbon nanotube–vitrimer composite for facile and efficient photo-welding of epoxy. Chemical Science, 2014, 5(9): 3486–3492
40. Berne D, Cuminet F, Lemouzy S, Joly-Duhamel C, Poli R, Caillol S, Leclerc E, Ladmiral V. Catalyst-free epoxy vitrimers based on transesterification internally activated by an α–CF3 Group. Macromolecules, 2022, 55(5): 1669–1679
41. Lu L, Jian P, Li G. Recyclable high-performance epoxy based on transesterification reaction. Journal of Materials Chemistry A: Materials for Energy and Sustainability, 2017, 5(40): 21505–21513
42. Xu Y, Dai S, Zhang H, Bi L, Jiang J, Chen Y. Reprocessable, self-adhesive, and recyclable carbon fiber-reinforced composites using a catalyst-free self-healing bio-based vitrimer matrix. ACS Sustainable Chemistry & Engineering, 2021, 9(48): 16281–16290
43. Liu Y, Tang Z, Chen Y, Zhang C, Guo B. Engineering of β-hydroxyl esters into elastomer–nanoparticle interface toward malleable, robust, and reprocessable vitrimer composites. ACS Applied Materials & Interfaces, 2018, 10(3): 2992–3001
44. Han J, Liu T, Hao C, Zhang S, Guo B, Zhang J. A catalyst-free epoxy vitrimer system based on multifunctional hyperbranched polymer.

Macromolecules, 2018, 51(17): 6789–6799
45. Yang Z, Wang Q, Wang T. Dual-triggered and thermally reconfigurable shape memory graphene-vitrimer composites. ACS Applied Materials & Interfaces, 2016, 8(33): 21691–21699
46. Reisinger D, Kaiser S, Rossegger E, Alabiso W, Rieger B, Schlögl S. Introduction of photolatent bases for locally controlling dynamic exchange reactions in thermo-activated vitrimers. Angewandte Chemie International Edition, 2021, 60(26): 14302–14306
47. Solouki Bonab V, Karimkhani V, Manas-Zloczower I. Ultra-fast microwave assisted self-healing of covalent adaptive polyurethane networks with carbon nanotubes. Macromolecular Materials and Engineering, 2019, 304(1): 1800405
48. Luo C, Yang W, Qi W, Chen Z, Lin J, Bian X, He S. Cost-efficient and recyclable epoxy vitrimer composite with low initial viscosity based on exchangeable disulfide crosslinks. Polymer Testing, 2022, 113: 107670
49. Azcune I, Huegun A, Ruiz de Luzuriaga A, Saiz E, Rekondo A. The effect of matrix on shape properties of aromatic disulfide based epoxy vitrimers. European Polymer Journal, 2021, 148: 110362
50. Zhou F, Guo Z, Wang W, Lei X, Zhang B, Zhang H, Zhang Q. Preparation of self-healing, recyclable epoxy resins and low-electrical resistance composites based on double-disulfide bond exchange. Composites Science and Technology, 2018, 167: 79–85
51. Fortman D J, Snyder R L, Sheppard D T, Dichtel W R. Rapidly reprocessable cross-linked poly-hydroxyurethanes based on disulfide exchange. ACS Macro Letters, 2018, 7(10): 1226–1231
52. Li W, Xiao L, Wang Y, Chen J, Nie X. Self-healing silicon-containing eugenol-based epoxy resin based on disulfide bond exchange: synthesis and structure-property relationships. Polymer, 2021, 229: 123967
53. Ma Z, Wang Y, Zhu J, Yu J, Hu Z. Bio-based epoxy vitrimers: reprocessibility, controllable shape memory, and degradability. Journal of Polymer Science Part A, Polymer Chemistry, 2017, 55(10): 1790–1799
54. Huang Z, Wang Y, Zhu J, Yu J, Hu Z. Surface engineering of nanosilica for vitrimer composites. Composites Science and Technology, 2018, 154: 18–27
55. Ben L, Zhu G, Hao Y, Ren T. An investigation on the performance of epoxy vitrimers based on disulfide bond. Journal of Applied Polymer Science, 2021, 139(5): 51589
56. Li Y, Feng H, Xiong J, Li L. A group-enriched viscoelastic model for high-damping vitrimers with many dangling chains. Materials, 2024, 17(20): 5062
57. Liu X, Song X, Chen B, Liu J, Feng Z, Zhang W, Zeng J, Liang L. Self-healing and shape-memory epoxy thermosets based on dynamic diselenide bonds. Reactive & Functional Polymers, 2022, 170: 105121
58. An X, Aguirresarobe R H, Irusta L, Ruipérez F, Matxain J M, Pan X, Aramburu N, Mecerreyes D, Sardon H, Zhu J. Aromatic diselenide crosslinkers to enhance the reprocessability and self-healing of polyurethane thermosets. Polymer Chemistry, 2017, 8(23): 3641–3646
59. Lyu L, Li D, Chen Y, Tian Y, Pei J. Dynamic chemistry based self-healing of asphalt modified by diselenide-crosslinked polyurethane elastomer. Construction & Building Materials, 2021, 293: 123480
60. Ji S, Cao W, Yu Y, Xu H. Visible-light-induced self-healing diselenide-containing polyurethane elastomer. Advanced Materials, 2015, 27(47): 7740–7745
61. Rashid M A, Zhu S, Zhang L, Jin K, Liu W. High-performance and fully recyclable epoxy resins cured by imine-containing hardeners derived from vanillin and syringaldehyde. European Polymer Journal, 2023, 187: 111878
62. Mai V D, Shin S R, Lee D S, Kang I. Thermal healing, reshaping and ecofriendly recycling of epoxy resin crosslinked with Schiff base of vanillin and hexane-1,6-diamine. Polymers, 2019, 11(2): 293
63. Yu Q, Peng X, Wang Y, Geng H, Xu A, Zhang X, Xu W, Ye D. Vanillin-based degradable epoxy vitrimers: reprocessability and mechanical properties study. European Polymer Journal, 2019, 117: 55–63
64. Denissen W, Rivero G, Nicolaÿ R, Leibler L, Winne J M, Du Prez F E. Vinylogous urethane vitrimers. Advanced Functional Materials, 2015, 25(16): 2451–2457
65. Wang S, Ma S, Li Q, Xu X, Wang B, Yuan W, Zhou S, You S, Zhu J. Facile *in situ* preparation of high-performance epoxy vitrimer from renewable resources and its application in nondestructive recyclable carbon fiber composite. Green Chemistry, 2019, 21(6): 1484–1497
66. Liu T, Hao C, Zhang S, Yang X, Wang L, Han J, Li Y, Xin J, Zhang J. A self-healable high glass transition temperature bioepoxy material based on vitrimer chemistry. Macromolecules, 2018, 51(15): 5577–5585
67. Niu X, Wang F, Li X, Zhang R, Wu Q, Sun P. Using Zn^{2+} ionomer to catalyze transesterification reaction in epoxy vitrimer. Industrial & Engineering Chemistry Research, 2019, 58(14): 5698–5706
68. Rashid M A, Zhu S, Jiang Q, Wei Y, Liu W. Developing easy processable, recyclable, and self-healable biobased epoxy resin through dynamic covalent imine bonds. ACS Applied Polymer Materials, 2023, 5(1): 279–289
69. Faghihnejad A, Feldman K E, Yu J, Tirrell M V, Israelachvili J N, Hawker C J, Kramer E J, Zeng H. Adhesion and surface interactions of a self-healing polymer with multiple hydrogen-bonding groups. Advanced Functional Materials, 2014, 24(16): 2322–2333
70. Xie Z, Hu B L, Li R W, Zhang Q. Hydrogen bonding in self-healing elastomers. ACS Omega, 2021, 6(14):

9319–9333
71. Zhou Z, Chen S, Xu X, Chen Y, Xu L, Zeng Y, Zhang F. Room temperature self-healing crosslinked elastomer constructed by dynamic urea bond and hydrogen bond. Progress in Organic Coatings, 2021, 154: 106213
72. Tamate R, Hashimoto K, Horii T, Hirasawa M, Li X, Shibayama M, Watanabe M. Self-healing micellar ion gels based on multiple hydrogen bonding. Advanced Materials, 2018, 30(36): 1802792
73. Shao C, Chang H, Wang M, Xu F, Yang J. High-strength, tough, and self-healing nanocomposite physical hydrogels based on the synergistic effects of dynamic hydrogen bond and dual coordination bonds. ACS Applied Materials & Interfaces, 2017, 9(34): 28305–28318
74. Krogsgaard M, Nue V, Birkedal H. Mussel-inspired materials: self-healing through coordination chemistry. Chemistry, 2016, 22(3): 844–857
75. Li C H, Zuo J L. Self-healing polymers based on coordination bonds. Advanced Materials, 2020, 32(27): 1903762
76. Lai J, Jia X, Wang D, Deng Y, Zheng P, Li C, Zuo J, Bao Z. Thermodynamically stable whilst kinetically labile coordination bonds lead to strong and tough self-healing polymers. Nature Communications, 2019, 10(1): 1164
77. Burattini S, Greenland B W, Merino D H, Weng W, Seppala J, Colquhoun H M, Hayes W, Mackay M E, Hamley I W, Rowan S J. A healable supramolecular polymer blend based on aromatic π–π stacking and hydrogen-bonding interactions. Journal of the American Chemical Society, 2010, 132(34): 12051–12058
78. Chen L, Zhao H B, Ni Y P, Fu T, Wu W S, Wang X L, Wang Y Z. 3D printable robust shape memory PET copolyesters with fire safety via π-stacking and synergistic crosslinking. Journal of Materials Chemistry A: Materials for Energy and Sustainability, 2019, 7(28): 17037–17045
79. Xiao W X, Fan C J, Li B, Liu W X, Yang K K, Wang Y Z. Single-walled carbon nanotubes as adaptable one-dimensional crosslinker to bridge multi-responsive shape memory network via π–π stacking. Composites Communications, 2019, 14: 48–54
80. Rodriguez E D, Luo X, Mather P T. Linear/network poly (ε-caprolactone) blends exhibiting shape memory assisted self-healing (SMASH). ACS Applied Materials & Interfaces, 2011, 3(2): 152–161
81. Zhang P, Li G. Advances in healing-on-demand polymers and polymer composites. Progress in Polymer Science, 2016, 57: 32–63
82. Li G, Uppu N. Shape memory polymer based self-healing syntactic foam: 3-D confined thermomechanical characterization. Composites Science and Technology, 2010, 70(9): 1419–1427
83. Li G, Nettles D. Thermomechanical characterization of a shape memory polymer based self-repairing syntactic foam. Polymer, 2010, 51(3): 755–762
84. Thakur V K, Kessler M R. Self-healing polymer nanocomposite materials: a review. Polymer, 2015, 69: 369–383
85. An X, Ding Y, Xu Y, Zhu J, Wei C, Pan X. Epoxy resin with exchangeable diselenide crosslinks to obtain reprocessable, repairable and recyclable fiber-reinforced thermoset composites. Reactive & Functional Polymers, 2022, 172: 105189
86. Zhang Q, Niu S, Wang L, Lopez J, Chen S, Cai Y, Du R, Liu Y, Lai J, Liu L, Li C, Yan X, Liu C, Tok J B H, Jia X, Bao Z. An elastic autonomous self-healing capacitive sensor based on a dynamic dual crosslinked chemical system. Advanced materials, 2018, 30(33): 1801435
87. Wang C, Bu Y, Guo S, Lu Y, Sun B, Shen Z. Self-healing cement composite: amine- and ammonium-based pH-sensitive superabsorbent polymers. Cement and Concrete Composites, 2019, 96: 154–162
88. Wang T, Zhang Y, Liu Q, Cheng W, Wang X, Pan L, Xu B, Xu H. A self-healable, highly stretchable, and solution processable conductive polymer composite for ultrasensitive strain and pressure sensing. Advanced Functional Materials, 2018, 28(7): 1705551
89. Xing L, Li Q, Zhang G, Zhang X, Liu F, Liu L, Huang Y, Wang Q. Self-healable polymer nanocomposites capable of simultaneously recovering multiple functionalities. Advanced Functional Materials, 2016, 26(20): 3524–3531
90. Zhang F, Ju P, Pan M, Zhang D, Huang Y, Li G, Li X. Self-healing mechanisms in smart protective coatings: a review. Corrosion Science, 2018, 144: 74–88
91. Yan D, Zhang Z, Zhang W, Wang Y, Zhang M, Zhang T, Wang J. Smart self-healing coating based on the highly dispersed silica/carbon nanotube nanomaterial for corrosion protection of steel. Progress in Organic Coatings, 2022, 164: 106694
92. Rezvani Ghomi E, Esmaeely Neisiany R, Nouri Khorasani S, Dinari M, Ataei S, Koochaki M S, Ramakrishna S. Development of an epoxy self-healing coating through the incorporation of acrylic acid-co-acrylamide copolymeric gel. Progress in Organic Coatings, 2020, 149: 105948
93. Lang S, Zhou Q. Synthesis and characterization of poly(urea-formaldehyde) microcapsules containing linseed oil for self-healing coating development. Progress in Organic Coatings, 2017, 105: 99–110
94. Nesterova T, Dam-Johansen K, Pedersen L T, Kiil S. Microcapsule-based self-healing anticorrosive coatings: capsule size, coating formulation, and exposure testing. Progress in Organic Coatings, 2012, 75(4): 309–318
95. Samadzadeh M, Boura S H, Peikari M, Kasiriha S M, Ashrafi A. A review on self-healing coatings based on micro/nanocapsules. Progress in Organic Coatings,

2010, 68(3): 159–164
96. Cho S H, White S R, Braun P V. Self-healing polymer coatings. Advanced Materials, 2009, 21(6): 645–649
97. Nguyen M T, Wang Z, Rod K A, Childers M I, Fernandez C, Koech P K, Bennett W D, Rousseau R, Glezakou V A. Atomic origins of the self-healing function in cement-polymer composites. ACS Applied Materials & Interfaces, 2018, 10(3): 3011–3019
98. Fernandez C A, Correa M, Nguyen M T, Rod K A, Dai G L, Cosimbescu L, Rousseau R, Glezakou V A. Progress and challenges in self-healing cementitious materials. Journal of Materials Science, 2021, 56(1): 201–230
99. Li X, Liu R, Li S, Zhang C, Yan J, Liu Y, Sun X, Su P. Properties and mechanism of self-healing cement paste containing microcapsule under different curing conditions. Construction & Building Materials, 2022, 357: 129410
100. Šovljanski O, Tomić A, Markov S. Relationship between bacterial contribution and self-healing effect of cement-based materials. Microorganisms, 2022, 10(7): 1399
101. Cavanagh P, Johnson C R, LeRoy-Delage S, DeBruijn G, Cooper I, Guillot D, Bulte V, Dargaud B. Self-healing cement—novel technology to achieve leak-free wells. In: SPE/IADC Drilling Conference. Amsterdam: The Society of Petroleum Engineers, 2007, SPE-105781-MS
102. Lucas S S, von Tapavicza M, Schmidt A M, Bertling J, Nellesen A. Study of quantification methods in self-healing ceramics, polymers and concrete: a route towards standardization. Journal of Intelligent Material Systems and Structures, 2016, 27(19): 2577–2598
103. Ozaki S, Nakamura M, Osada T. Finite element analysis of the fracture statistics of self-healing ceramics. Science and Technology of Advanced Materials, 2020, 21(1): 609–625
104. Ozaki S, Yamamoto J, Kanda N, Osada T. Kinetics-based constitutive model for self-healing ceramics and its application to finite element analysis of Alumina/SiC composites. Open Ceramics, 2021, 6: 100135
105. Tinnefeld P, Cordes T. 'Self-healing'dyes: intramolecular stabilization of organic fluorophores. Nature Methods, 2012, 9(5): 426–427
106. van der Velde J H M, Smit J H, Hebisch E, Trauschke V, Punter M, Cordes T. Self-healing dyes for super-resolution fluorescence microscopy. Journal of Physics D: Applied Physics, 2019, 52(3): 034001
107. Seifan M, Samani A K, Berenjian A. Bioconcrete: next generation of self-healing concrete. Applied Microbiology and Biotechnology, 2016, 100(6): 2591–2602
108. Amirreza T, Abd M M Z. A review of self-healing concrete research development. Journal of Environmental Treatment Techniques, 2014, 2(1): 1–11
109. De Belie N, Gruyaert E, Al-Tabbaa A, Antonaci P, Baera C, Bajare D, Darquennes A, Davies R, Ferrara L, Jefferson T, Litina C, Miljevic B, Otlewska A, Ranogajec J, Roig-Flores M, Paine K, Lukowski P, Serna P, Tulliani J M, Vucetic S, Wang J, Jonkers H M. A review of self-healing concrete for damage management of structures. Advanced Materials Interfaces, 2018, 5(17): 1800074
110. Yin H, Song P, Chen X, Huang Q, Huang H. A self-healing hydrogel based on oxidized microcrystalline cellulose and carboxymethyl chitosan as wound dressing material. International Journal of Biological Macromolecules, 2022, 221: 1606–1617
111. Mou C, Wang X, Teng J, Xie Z, Zheng M. Injectable self-healing hydrogel fabricated from antibacterial carbon dots and ε-polylysine for promoting bacteria-infected wound healing. Journal of Nanobiotechnology, 2022, 20(1): 368
112. Huang X, Tang L, Xu L, Zhang Y, Li G, Peng W, Guo X, Zhou L, Liu C, Shen X C. A NIR-II light-modulated injectable self-healing hydrogel for synergistic photothermal/chemodynamic/chemotherapy of melanoma and wound healing promotion. Journal of Materials Chemistry B: Materials for Biology and Medicine, 2022, 10(38): 7717–7731
113. Jiang X, Yan N, Wang M, Feng M, Guan Q, Xu L. Magnetic nanostructure and biomolecule synergistically promoted Suaeda-inspired self-healing hydrogel composite for seawater evaporation. Science of the Total Environment, 2022, 830: 154545
114. Yang Y, Sun H, Shi C, Liu Y, Zhu Y, Song Y. Self-healing hydrogel with multiple adhesion as sensors for winter sports. Journal of Colloid and Interface Science, 2023, 629: 1021–1031
115. Lakes R S. Viscoelastic Materials. Cambridge: Cambridge University Press, 2009, 50–59
116. Wang H, Su Z, Li C. Design and synthesis of highly stretchable self-healing materials. Science Bulletin, 2020, 65(1): 37–52
117. Bert C W. Material damping: An introductory review of mathematic measures and experimental technique. Journal of Sound and Vibration, 1973, 29(2): 129–153
118. Ashby M F. Overview No. 80: on the engineering properties of materials. Acta Metallurgica, 1989, 37(5): 1273–1293
119. Treviso A, Van Genechten B, Mundo D, Tournour M. Damping in composite materials: properties and models. Composites Part B: Engineering, 2015, 78: 144–152
120. Barkaoui A, Hambli R. Finite element 3D modeling of mechanical behavior of mineralized collagen microfibrils. Journal of Applied Biomaterials & Biomechanics, 2011, 9(3): 199–206
121. Haque M A, Kurokawa T, Gong J P. Super tough

double network hydrogels and their application as biomaterials. Polymer, 2012, 53(9): 1805–1822
122. Khiêm V N, Mai T T, Urayama K, Gong J P, Itskov M. A multiaxial theory of double network hydrogels. Macromolecules, 2019, 52(15): 5937–5947
123. Na Y H, Katsuyama Y, Kuwabara R, Kurokawa T, Osada Y, Shibayama M, Gong J P. Toughening of hydrogels with double network structure. Journal of Surface Science and Nanotechnology, 2005, 3: 8–11
124. Nakajima T, Furukawa H, Gong J P, Lin E K, Wu W L. A deformation mechanism for double-network hydrogels with enhanced toughness. Macromolecular Symposia, 2010, 291–292(1): 122–126
125. Ni X, Putra A, Furukawa H, Gong J P. Synthesis of novel double network hydrogels via atom transfer radical polymerization. Composite Interfaces, 2009, 16(4–6): 433–446
126. Yasuda K, Gong J P, Katsuyama Y, Nakayama A, Tanabe Y, Kondo E, Ueno M, Osada Y. Biomechanical properties of high-toughness double network hydrogels. Biomaterials, 2004, 26(21): 4468–4475
127. Suhr J, Koratkar N, Keblinski P, Ajayan P. Viscoelasticity in carbon nanotube composites. Nature Materials, 2005, 4(2): 134–137
128. Koratkar N, Wei B Q, Ajayan P M. Carbon nanotube films for damping applications. Advanced Materials, 2002, 14(13–14): 997–1000
129. Wang S, Teng N, Dai J, Liu J, Cao L, Zhao W, Liu X. Taking advantages of intramolecular hydrogen bonding to prepare mechanically robust and catalyst-free vitrimer. Polymer, 2020, 210: 123004
130. Belowich M E, Stoddart J F. Dynamic imine chemistry. Chemical Society Reviews, 2012, 41(6): 2003–2024
131. Huang Z, Wang F, Zhao H, Li C. Study on the preparation and repair performance of epoxy resin/polyethylene wax two-phase self repair material. Journal of Chongqing University of Technology, 2021, 35(4): 111–116 (in Chinese)
132. Cordier P, Tournilhac F, Soulié-Ziakovic C, Leibler L. Self-healing and thermoreversible rubber from supramolecular assembly. Nature, 2008, 451(7181): 977–980
133. Tee B C K, Wang C, Allen R, Bao Z. An electrically and mechanically self-healing composite with pressure- and flexion-sensitive properties for electronic skin applications. Nature Nanotechnology, 2012, 7(12): 825–832
134. Lin Y, Li G. An intermolecular quadruple hydrogen-bonding strategy to fabricate self-healing and highly deformable polyurethane hydrogels. Journal of Materials Chemistry B: Materials for Biology and Medicine, 2014, 2(39): 6878–6885
135. Guadagno L, Vertuccio L, Naddeo C, Calabrese E, Barra G, Raimondo M, Sorrentino A, Binder W H, Michael P, Rana S. Self-healing epoxy nanocomposites via reversible hydrogen bonding. Composites Part B: Engineering, 2019, 157: 1–13
136. Cheng Y, Zhang L, Hu R, Wang Y, Jin X, Qiu S, Zhang H, Jiang D. Preparation and characterization of hydrogen-bonded carbon nanotubes reinforced self-healing composites. Chinese Journal of Applied Chemistry, 2020, 37(10): 1147–1155 (in Chinese)
137. Jia X Y, Mei J F, Lai J C, Li C H, You X Z. A highly stretchable polymer that can be thermally healed at mild temperature. Macromolecular Rapid Communications, 2016, 37(12): 952–956
138. Wang Z, Xie C, Yu C, Fei G, Wang Z, Xia H. A facile strategy for self-healing polyurethanes containing multiple metal–ligand bonds. Macromolecular Rapid Communications, 2018, 39(6): 1700678
139. Weng L, Gouldstone A, Wu Y, Chen W. Mechanically strong double network photocrosslinked hydrogels from N,N-dimethylacrylamide and glycidyl methacrylated hyaluronan. Biomaterials, 2008, 29(14): 2153–2163
140. Dai T, Qing X, Wang J, Shen C, Lu Y. Interfacial polymerization to high-quality polyacrylamide/polyaniline composite hydrogels. Composites Science and Technology, 2010, 70(3): 498–503
141. Hu J, Hiwatashi K, Kurokawa T, Liang S M, Wu Z L, Gong J P. Microgel-reinforced hydrogel films with high mechanical strength and their visible mesoscale fracture structure. Macromolecules, 2011, 44(19): 7775–7781
142. Cao Y, Fan D, Lin S, Ng F T T, Pan Q. Branched alkylated polynorbornene and 3D flower-like MoS_2 nanospheres reinforced phase change composites with high thermal energy storage capacity and photothermal conversion efficiency. Renewable Energy, 2021, 179: 687–695
143. Demir E, Güler Ö. Production and properties of epoxy matrix composite reinforced with hollow silica nanospheres (HSN): mechanical, thermal insulation, and sound insulation properties. Journal of Polymer Research, 2022, 29(11): 477
144. Zangiabadi Z, Hadianfard M J. The role of hollow silica nanospheres and rigid silica nanoparticles on acoustic wave absorption of flexible polyurethane foam nanocomposites. Journal of Cellular Plastics, 2020, 56(4): 395–410
145. Sun Y, Wu H, Li M, Meng Q, Gao K, Lu X, Liu B. The effect of ZrO_2 nanoparticles on the microstructure and properties of sintered WC–bronze-based diamond composites. Materials, 2016, 9(5): 343
146. Chellvarajoo S, Abdullah M Z, Khor C Y. Effects of diamond nanoparticles reinforcement into lead-free Sn–3.0Ag–0.5Cu solder pastes on microstructure and mechanical properties after reflow soldering process. Materials & Design, 2015, 82: 206–215
147. Saba F, Zhang F, Liu S, Liu T. Reinforcement size

dependence of mechanical properties and strengthening mechanisms in diamond reinforced titanium metal matrix composites. Composites Part B: Engineering, 2019, 167: 7–19
148. Zhang H, Gao C, Li H, Pang F, Zou T, Wang H, Wang N. Analysis of functionally graded carbon nanotube-reinforced composite structures: a review. Nanotechnology Reviews, 2020, 9(1): 1408–1426
149. Bal S, Samal S S. Carbon nanotube reinforced polymer composites—a state of the art. Bulletin of Materials Science, 2007, 30(4): 379–386
150. Mohd Nurazzi N, Asyraf M R M, Khalina A, Abdullah N, Sabaruddin F A, Kamarudin S H, Ahmad S, Mahat A M, Lee C L, Aisyah H A, Norrrahim M N F, Ilyas R A, Harussani M M, Ishak M R, Sapuan S M. Fabrication, functionalization, and application of carbon nanotube-reinforced polymer composite: an overview. Polymers, 2021, 13(7): 1047
151. Li L, Chen Y, Stachurski Z H. Boron nitride nanotube reinforced polyurethane composites. Progress in Natural Science, 2013, 23(2): 170–173
152. Bansal N P, Hurst J B, Choi S R. Boron nitride nanotubes-reinforced glass composites. Journal of the American Ceramic Society, 2006, 89(1): 388–390
153. Wang W L, Bi J Q, Wang S R, Sun K N, Du M, Long N N, Bai Y J. Microstructure and mechanical properties of alumina ceramics reinforced by boron nitride nanotubes. Journal of the European Ceramic Society, 2011, 31(13): 2277–2284
154. Kumar H G P, Xavior M A, 0. Graphene reinforced metal matrix composite (GRMMC): a review. Procedia Engineering, 2014, 97: 1033–1040
155. Young R J, Kinloch I A, Gong L, Novoselov K S. The mechanics of graphene nanocomposites: a review. Composites Science and Technology, 2012, 72(12): 1459–1476
156. Güler Ö, Bağcı N. A short review on mechanical properties of graphene reinforced metal matrix composites. Journal of Materials Research and Technology, 2020, 9(3): 6808–6833
157. Gong K, Pan Z, Korayem A H, Qiu L, Li D, Collins F, Wang C M, Duan W H. Reinforcing effects of graphene oxide on portland cement paste. Journal of Materials in Civil Engineering, 2015, 27(2): A4014010
158. Mensah B, Kim S, Arepalli S, Nah C. A study of graphene oxide-reinforced rubber nanocomposite. Journal of Applied Polymer Science, 2014, 131(16): 40640
159. Zhou Z, Yang Z, Liu C. Novel nanocomposite super absorbent polymers reinforced by clay nanosheets. Russian Journal of Applied Chemistry, 2016, 89(2): 324–329
160. Sedush N G, Kadina Y A, Razuvaeva E V, Puchkov A A, Shirokova E M, Gomzyak V I, Kalinin K T, Kulebyakina A I, Chvalun S N. Nanoformulations of drugs based on biodegradable lactide copolymers with various molecular structures and architectures. Nanobiotechnology Reports, 2021, 16(4): 421–438
161. Kallumottakkal M, Hussein M I, Haik Y, Abdul Latef T B. Functionalized-CNT polymer composite for microwave and electromagnetic shielding. Polymers, 2021, 13(22): 3907
162. You X, Feng Q, Yang J, Huang K, Hu J, Dong S. Preparation of high concentration graphene dispersion with low boiling point solvents. Journal of Nanoparticle Research, 2019, 21: 1–11
163. Gardea F, Glaz B, Riddick J, Lagoudas D C, Naraghi M. Energy dissipation due to interfacial slip in nanocomposites reinforced with aligned carbon nanotubes. ACS Applied Materials & Interfaces, 2015, 7(18): 9725–9735
164. Barabanova A I, Afanas'ev E S, Molchanov V S, Askadskii A A, Philippova O E. Unmodified silica nanoparticles enhance mechanical properties and welding ability of epoxy thermosets with tunable vitrimer matrix. Polymers, 2021, 13(18): 3040
165. Atif R, Inam F. Modeling and simulation of graphene based polymer nanocomposites: advances in the last decade. Graphene, 2016, 5(2): 96–142
166. Katsiropoulos C V, Pappas P, Koutroumanis N, Kokkinos A, Galiotis C. Enhancement of damping response in polymers and composites by the addition of graphene nanoplatelets. Composites Science and Technology, 2022, 227: 109562
167. Li Y, Gao F, Xue Z, Luan Y, Yan X, Guo Z, Wang Z. Synergistic effect of different graphene-CNT heterostructures on mechanical and self-healing properties of thermoplastic polyurethane composites. Materials & Design, 2018, 137: 438–445
168. Kumar P, Kucherov L, Ryvkin M. Fracture toughness of self-similar hierarchical material. International Journal of Solids and Structures, 2020, 203: 210–223
169. Dyskin A V. Effective characteristics and stress concentrations in materials with self-similar microstructure. International Journal of Solids and Structures, 2005, 42(2): 477–502
170. Claussen K U, Scheibel T, Schmidt H W, Giesa R. Polymer gradient materials: Can nature teach us new tricks? Macromolecular Materials and Engineering, 2012, 297(10): 938–957
171. Wei Z, Xu X. Gradient design of bio-inspired nacre-like composites for improved impact resistance. Composites Part B: Engineering, 2021, 215: 108830
172. Liu Z, Meyers M A, Zhang Z, Ritchie R O. Functional gradients and heterogeneities in biological materials: design principles, functions, and bioinspired applications. Progress in Materials Science, 2017, 88: 467–498
173. Meyers M A, Lin A Y M, Chen P Y, Muyco J. Mechanical strength of abalone nacre: role of the soft organic layer. Journal of the Mechanical Behavior of Biomedical Materials, 2008, 1(1): 76–85

174. Meyers M A, Chen P Y, Lin A Y M, Seki Y. Biological materials: Structure and mechanical properties. Progress in Materials Science, 2008, 53(1): 1–206
175. Wegst U G K, Bai H, Saiz E, Tomsia A P, Ritchie R O. Bioinspired structural materials. Nature Materials, 2015, 14(1): 23–36
176. Xu A W, Antonietti M, Yu S H, Cölfen H. Polymer-mediated mineralization and self-similar mesoscale-organized calcium carbonate with unusual superstructures. Advanced Materials, 2008, 20(7): 1333–1338
177. Pragya A, Ghosh T K. Soft functionally gradient materials and structures – natural and manmade: a review. Advanced Materials, 2023, 35(49): 2300912
178. Singh S, Pal K. Investigation on microstructural, mechanical and damping properties of SiC/TiO_2, $SiC/Li_4Ti_5O_{12}$ reinforced Al matrix. Ceramics International, 2021, 47(10): 14809–14820
179. Sohn M S, Kim K S, Hong S H, Kim J K. Dynamic mechanical properties of particle-reinforced EPDM composites. Journal of Applied Polymer Science, 2003, 87(10): 1595–1601
180. Madarvoni S, PS Rama S. Dynamic mechanical behaviour of graphene, hexagonal boron nitride reinforced carbon-kevlar, hybrid fabric-based epoxy nanocomposites. Polymers & Polymer Composites, 2022, 30: 09673911221107289
181. Yu S, Hing P. Dynamic mechanical properties of polystyrene–aluminum nitride composite. Journal of Applied Polymer Science, 2000, 78(7): 1348–1353
182. Madeira S, Carvalho O, Carneiro V H, Soares D, Silva F S, Miranda G. Damping capacity and dynamic modulus of hot pressed AlSi composites reinforced with different SiC particle sized. Composites Part B: Engineering, 2016, 90: 399–405
183. Dong H, Zhang G, Jiang Y, Zhang Y. Effects of boron nitride and carbon nanotube on damping properties, thermal conductivity and compression stress relaxation behavior of BIIR. Polymer Composites, 2022, 43(2): 1128–1135
184. Li G, Fan X, Deng D, Wu Q H, Jia L. Surface charge induced self-assembled nest-like Ni_3S_2/PNG composites for high-performance supercapacitors. Journal of Colloid and Interface Science, 2023, 650: 913–923
185. Zhou J, Xie C, Xu H, Gou B, Zhong A, Zhang D, Cai H, Bi C, Li L, Wang R. Self-assembled nest-like BN skeletons enable polymer composites with high thermal management capacity. Composites Science and Technology, 2024, 258: 110869
186. Li Y, Cai S, Huang X. Multi-scaled enhancement of damping property for carbon fiber reinforced composites. Composites Science and Technology, 2017, 143: 89–97
187. Mofokeng J P, Luyt A S, Tábi T, Kovács J. Comparison of injection moulded, natural fibre-reinforced composites with PP and PLA as matrices. Journal of Thermoplastic Composite Materials, 2012, 25(8): 927–948
188. Sordo F, Michaud V. Processing and damage recovery of intrinsic self-healing glass fiber reinforced composites. Smart Materials and Structures, 2016, 25(8): 084012
189. Khan N I, Halder S. Self-healing fiber-reinforced polymer composites for their potential structural applications. In: Thomas and Surendran eds. Self-Healing Polymer-Based Systems. Elsevier, 2020, 455–472
190. Wu X, Yu H, Wang L, Gong X, Chen D, Hong Y, Zhang Y. Construction of three-dimensional interconnected boron nitride/sliver networks within epoxy composites for enhanced thermal conductivity. Composites Science and Technology, 2023, 243: 110268
191. Maiti S, Islam M R, Uddin M A, Afroj S, Eichhorn S J, Karim N. Sustainable fiber-reinforced composites: a review. Advanced Sustainable Systems, 2022, 6(11): 2200258
192. Drach A, Drach B, Tsukrov I. Processing of fiber architecture data for finite element modeling of 3D woven composites. Advances in Engineering Software, 2014, 72: 18–27
193. Chen S M, Gao H L, Zhu Y B, Yao H B, Mao L B, Song Q Y, Xia J, Pan Z, He Z, Wu H A, Yu S H. Biomimetic twisted plywood structural materials. National Science Review, 2018, 5(5): 703–714
194. Ni X, Furtado C, Kalfon-Cohen E, Zhou Y, Valdes G A, Hank T J, Camanho P P, Wardle B L. Static and fatigue interlaminar shear reinforcement in aligned carbon nanotube-reinforced hierarchical advanced composites. Composites Part A: Applied Science and Manufacturing, 2019, 120: 106–115
195. Zhu J, Zhou H, Wang C, Zhou L, Yuan S, Zhang W. A review of topology optimization for additive manufacturing: status and challenges. Chinese Journal of Aeronautics, 2021, 34(1): 91–110
196. Jiang H, Ren Y, Liu Z, Zhang S, Lin Z. Low-velocity impact resistance behaviors of bio-inspired helicoidal composite laminates with non-linear rotation angle based layups. Composite Structures, 2019, 214: 463–475
197. Xiang Y, Huang Y, Lu J, Yuan L, Zou S. New matrix method for analyzing vibration and damping effect of sandwich circular cylindrical shell with viscoelastic core. Applied Mathematics and Mechanics, 2008, 29(12): 1587–1600
198. Loredo A, Plessy A, El Hafidi A, Hamzaoui N. Numerical vibroacoustic analysis of plates with constrained-layer damping patches. Journal of the Acoustical Society of America, 2011, 129(4): 1905–1918
199. McDaniel J G, Magliula E A. Analysis and

optimization of constrained layer damping treatments using a semi-analytical finite element method. Proceedings of Meetings on Acoustics, 2013, 19(1): 065022

200. Xie Z, Shepard W S. Development of a new finite element and parametric study for plates with compressible constrained layer damping. Journal of Composite Materials, 2012, 46(11): 1263–1273
201. Pan J, Liu Z, Kou X, Song Q. Constrained layer damping treatment of a model support sting. Chinese Journal of Aeronautics, 2021, 34(8): 58–64
202. Khalfi B, Nasraoui M T, Chakhari J, Ross A, Chafra M. Dynamic behavior of cylindrical shell with partial constrained viscoelastic layer damping under an impact load. Acta Mechanica, 2023, 234(5): 2125–2143
203. Madeira J F A, Araújo A L, Mota Soares C M. Multiobjective optimization of constrained layer damping treatments in composite plate structures. Mechanics of Advanced Materials and Structures, 2017, 24(5): 427–436
204. Zhang D, Wu Y, Lu X, Zheng L. Topology optimization of constrained layer damping plates with frequency-and temperature-dependent viscoelastic core via parametric level set method. Mechanics of Advanced Materials and Structures, 2022, 29(1): 154–170
205. Plisson J. Periodic and locally resonant waveguides for vibration control in an industrial context. Dissertation for the Doctoral Degree. Le Mans: Le Mans Université, 2021, 5–7
206. Bacquet C L, Al Ba'ba'a H, Frazier M J, Nouh M, Hussein M I. Metadamping: dissipation emergence in elastic metamaterials. Advances in Applied Mechanics, 2018, 51: 115–164
207. Mei C, Li L, Li X, Jiang Y, Han X, Tang H, Wang X, Hu Y. Spatiotemporal damping of dissipative metamaterial. International Journal of Mechanical Sciences, 2023, 254: 108393
208. Garg A, Sharma A, Zheng W, Li L. Dactyl club and nacre-inspired impact resistant behavior of layered structures: a review of present trends and prospects. Materials Today Communications, 2024, 41: 110553
209. Li S, Zheng W, Li L. Spatiotemporally nonlocal homogenization method for viscoelastic porous metamaterial structures. International Journal of Mechanical Sciences, 2024, 282: 109572
210. Xiong J, Ma L, Stocchi A, Yang J, Wu L, Pan S. Bending response of carbon fiber composite sandwich beams with three dimensional honeycomb cores. Composite Structures, 2014, 108: 234–242
211. Xiong J, Ma L, Vaziri A, Yang J, Wu L. Mechanical behavior of carbon fiber composite lattice core sandwich panels fabricated by laser cutting. Acta Materialia, 2012, 60(13–14): 5322–5334
212. Yang J S, Li D L, Ma L, Zhang S Q, Schröder K U, Schmidt R. Numerical static and dynamic analyses of improved equivalent models for corrugated sandwich structures. Mechanics of Advanced Materials and Structures, 2019, 26(18): 1556–1567
213. Yang J S, Yang F, Han L, Yang L H, Wu L Z. Vibration response of glass fiber composite multi-layer graded corrugated sandwich panels. Journal of Sandwich Structures & Materials, 2022, 24(2): 1491–1511
214. Zhang G, Wang B, Ma L, Wu L, Pan S, Yang J. Energy absorption and low velocity impact response of polyurethane foam filled pyramidal lattice core sandwich panels. Composite Structures, 2014, 108: 304–310
215. Wei Y, Li H, Yang H, Ma Y, Cheng J, Gao P, Shi J, Yu B, Lin F. Damping and mechanical properties of epoxy/316L metallic lattice composites. Materials, 2022, 16(1): 130
216. Xu Z, Ha C S, Kadam R, Lindahl J, Kim S, Wu H F, Kunc V, Zheng X. Additive manufacturing of two-phase lightweight, stiff and high damping carbon fiber reinforced polymer microlattices. Additive Manufacturing, 2020, 32: 101106
217. Yin H, Zhang W, Zhu L, Meng F, Liu J, Wen G. Review on lattice structures for energy absorption properties. Composite Structures, 2023, 304: 116397
218. Yi Y M, Park S H, Youn S K. Design of microstructures of viscoelastic composites for optimal damping characteristics. International Journal of Solids and Structures, 2000, 37(35): 4791–4810
219. Zhang H, Ding X, Li H, Xiong M. Multi-scale structural topology optimization of free-layer damping structures with damping composite materials. Composite Structures, 2019, 212: 609–624
220. Wu F, Zhang X, Xue P, Zahran M S. Multi-scale concurrent topology optimization of frequency-and temperature-dependent viscoelastic structures for enhanced damping performance. Structural and Multidisciplinary Optimization, 2023, 66(11): 234
221. Ma J, Zhang X, Kang Z. Directional damping design of viscoelastic composites via topology optimization. International Journal of Mechanical Sciences, 2024, 275: 109300
222. Zhang X, Kang Z. Vibration suppression using integrated topology optimization of host structures and damping layers. Journal of Vibration and Control, 2016, 22(1): 60–76
223. Bessa M A, Glowacki P, Houlder M. Bayesian machine learning in metamaterial design: fragile becomes supercompressible. Advanced Materials, 2019, 31(48): 1904845
224. Muhammad, Kennedy J, Lim C W. Machine learning and deep learning in phononic crystals and metamaterials – a review. Materials Today Communications, 2022, 33: 104606
225. Chatterjee T, Bera K K, Banerjee A. Machine learning enabled quantification of stochastic active

metadamping in acoustic metamaterials. Journal of Sound and Vibration, 2023, 567: 117938
226. Challapalli A, Konlan J, Patel D, Li G. Discovery of cellular unit cells with high natural frequency and energy absorption capabilities by an inverse machine learning framework. Frontiers in Mechanical Engineering, 2021, 7: 779098
227. Abu-Mualla M, Huang J. Inverse design of 3D cellular materials with physics-guided machine learning. Materials & Design, 2023, 232: 112103
228. Bastek J H, Kochmann D M. Inverse design of nonlinear mechanical metamaterials via video denoising diffusion models. Nature Machine Intelligence, 2023, 5(12): 1466–1475
229. Kang S, Song H, Seok Kang H, Bae B S, Ryu S. Customizable metamaterial design for desired strain-dependent Poisson's ratio using constrained generative inverse design network. Materials & Design, 2024, 247: 113377
230. Xu M, Cheng B, Sheng Y, Zhou J, Wang M, Jiang X, Lu X. High-performance cross-linked self-healing material based on multiple dynamic bonds. ACS Applied Polymer Materials, 2020, 2(6): 2228–2237
231. Zhang W, Wang M, Zhou J, Sheng Y, Xu M, Jiang X, Ma Y, Lu X. Preparation of room-temperature self-healing elastomers with high strength based on multiple dynamic bonds. European Polymer Journal, 2021, 156: 110614
232. Song F, Li Z, Jia P, Zhang M, Bo C, Feng G, Hu L, Zhou Y. Tunable "soft and stiff", self-healing, recyclable, thermadapt shape memory biomass polymers based on multiple hydrogen bonds and dynamic imine bonds. Journal of Materials Chemistry A: Materials for Energy and Sustainability, 2019, 7(21): 13400–13410
233. Zhu X, Zhang W, Lu G, Zhao H, Wang L. Ultrahigh mechanical strength and robust room-temperature self-healing properties of a polyurethane–graphene oxide network resulting from multiple dynamic bonds. ACS Nano, 2022, 16(10): 16724–16735
234. Jiang Z, Bhaskaran A, Aitken H M, Shackleford I C G, Connal L A. Using synergistic multiple dynamic bonds to construct polymers with engineered properties. Macromolecular Rapid Communications, 2019, 40(10): 1900038
235. Kim G, Caglayan C, Yun G J. Epoxy-based catalyst-free self-healing elastomers at room temperature employing aromatic disulfide and hydrogen bonds. ACS Omega, 2022, 7(49): 44750–44761
236. Martinez-Diaz D, Cortés A, Jiménez-Suárez A, Prolongo S G. Hardener isomerism and content of dynamic disulfide bond effect on chemical recycling of epoxy networks. ACS Applied Polymer Materials, 2022, 4(7): 5068–5076
237. Segurado J, LLorca J. A computational micromechanics study of the effect of interface decohesion on the mechanical behavior of composites. Acta Materialia, 2005, 53(18): 4931–4942
238. Jasiuk Iwona M, Tong Y. Effect of interface on the elastic stiffness of composites. American Society of Mechanical Engineers. Applied Mechanics Division, AMD, 1989, 100: 49–54
239. Tarrés Q, Hernández-Díaz D, Ardanuy M. Interface strength and fiber content influence on corn stover fibers reinforced bio-polyethylene composites stiffness. Polymers, 2021, 13(5): 768
240. Xu X, Li B, Lu H, Zhang Z, Wang H. The interface structure of nano-SiO_2/PA66 composites and its influence on material's mechanical and thermal properties. Applied Surface Science, 2007, 254(5): 1456–1462
241. Greszczuk L B. Theoretical Studies of the Mechanics of the Fiber-Matrix Interface in Composites. ASTM International, 1969, 42–58
242. Li S, Wang K, Zhu W, Peng Y, Ahzi S, Chinesta F. Contributions of interfaces on the mechanical behavior of 3D printed continuous fiber reinforced composites. Construction & Building Materials, 2022, 340: 127842
243. Lee S, Jung J, Ryu S. Applicability of interface spring and interphase models in micromechanics for predicting effective stiffness of polymer-matrix nanocomposite. Extreme Mechanics Letters, 2021, 49: 101489
244. Demir B, Henderson L C, Walsh T R. Design rules for enhanced interfacial shear response in functionalized carbon fiber epoxy composites. ACS Applied Materials & Interfaces, 2017, 9(13): 11846–11857
245. Guru K, Sharma T, Shukla K K, Mishra S B. Effect of interface on the elastic modulus of CNT nanocomposites. Journal of Nanomechanics & Micromechanics, 2016, 6(3): 04016004
246. Duan K, Li Y, Li L, Hu Y, Wang X. Pillared graphene as excellent reinforcement for polymer-based nanocomposites. Materials & Design, 2018, 147: 11–18
247. Sluysmans D, Stoddart J F. The burgeoning of mechanically interlocked molecules in chemistry. Trends in Chemistry, 2019, 1(2): 185–197
248. Schröder H V, Zhang Y, Link A J. Dynamic covalent self-assembly of mechanically interlocked molecules solely made from peptides. Nature Chemistry, 2021, 13(9): 850–857
249. Kim K. Mechanically interlocked molecules incorporating cucurbituril and their supramolecular assemblies. Chemical Society Reviews, 2002, 31(2): 96–107
250. Heard A W, Goldup S M. Simplicity in the design, operation, and applications of mechanically interlocked molecular machines. ACS Central Science, 2020, 6(2): 117–128
251. Leigh D A, Wong J K Y, Dehez F, Zerbetto F. Unidirectional rotation in a mechanically interlocked molecular rotor. Nature, 2003, 424(6945): 174–179

252. Chen L, Sheng X, Li G, Huang F. Mechanically interlocked polymers based on rotaxanes. Chemical Society Reviews, 2022, 51(16): 7046–7065
253. Zhao J, Zhang Z, Cheng L, Bai R, Zhao D, Wang Y, Yu W, Yan X. Mechanically interlocked vitrimers. Journal of the American Chemical Society, 2021, 144(2): 872–882
254. Shokuhfar A, Arab B. The effect of cross linking density on the mechanical properties and structure of the epoxy polymers: molecular dynamics simulation. Journal of Molecular Modeling, 2013, 19(9): 3719–3731
255. Urbaczewski-Espuche E, Galy J, Gerard J F, Pascault J P, Sautereau H. Influence of chain flexibility and crosslink density on mechanical properties of epoxy/amine networks. Polymer Engineering and Science, 1991, 31(22): 1572–1580
256. Kim B, Choi J, Yang S, Yu S, Cho M. Influence of crosslink density on the interfacial characteristics of epoxy nanocomposites. Polymer, 2015, 60: 186–197
257. Bandyopadhyay A, Valavala P K, Clancy T C, Wise K E, Odegard G M. Molecular modeling of crosslinked epoxy polymers: the effect of crosslink density on thermomechanical properties. Polymer, 2011, 52(11): 2445–2452
258. Isogai T, Hayashi M. Critical effects of branch numbers at the cross-link point on the relaxation behaviors of transesterification vitrimers. Macromolecules, 2022, 55(15): 6661–6670
259. Hajj R, Duval A, Dhers S, Avérous L. Network design to control polyimine vitrimer properties: physical versus chemical approach. Macromolecules, 2020, 53(10): 3796–3805
260. Grunlan M A, Fei R, George J T, Means A K. High strength thermoresponsive double network hydrogels. In: Abstracts of Papers of the American Chemical Society. ACS, 2013, 245
261. Zhu D, Miao M, Du X, Peng Y, Wang Z, Liu S, Xing J. Long/short chain crosslinkers-optimized and PEDOT:PSS-enhanced covalent double network hydrogels rapidly prepared under green LED irradiation as flexible strain sensor. European Polymer Journal, 2022, 174: 111327
262. Grunlan M, Kristen M A. Double network hydrogels with high stiffness and ultra-high strength. In: Abstracts of Papers of the American Chemical Society. ACS, 2018, 255
263. Li X, Wang Y, Li D, Shu M, Shang L, Xia M, Huang Y. High-strength, thermosensitive double network hydrogels with antibacterial functionality. Soft Matter, 2021, 17(28): 6688–6696
264. Jia Y, Zhou Z, Jiang H, Liu Z. Characterization of fracture toughness and damage zone of double network hydrogels. Journal of the Mechanics and Physics of Solids, 2022, 169: 105090
265. Chen Q, Chen H, Zhu L, Zheng J. Engineering of tough double network hydrogels. Macromolecular Chemistry and Physics, 2016, 217(9): 1022–1036
266. Reznikov N, Bilton M, Lari L, Stevens M M, Kröger R. Fractal-like hierarchical organization of bone begins at the nanoscale. Science, 2018, 360(6388): eaao2189
267. Feng H, Xu C, Xiao L, Li L. Multiscale hierarchical composite with extremely specific damping performance via bottom-up synergistic enhancement strategy. Virtual and Physical Prototyping, 2025, 20(1): e2448541